NASA Technical Paper 2361

1984

Design Guidelines for Assessing and Controlling Spacecraft Charging Effects

Carolyn K. Purvis
Lewis Research Center
Cleveland, Ohio

Henry B. Garrett
and A. C. Whittlesey
California Institute of Technology
Jet Propulsion Laboratory
Pasadena, California

N. John Stevens
Hughes Aircraft Company
El Segundo, California

National Aeronautics
and Space Administration

Scientific and Technical Information Branch

Foreword

Experience has indicated a need for uniform criteria, or guidelines, to be used in all phases of spacecraft design. Accordingly, guidelines have been developed for the control of absolute and differential charging of spacecraft surfaces by the lower energy (less than approximately 50 keV) space charged-particle environment. Interior charging due to higher energy particles was not considered.

This document is to be regarded as a guide to good design practices for assessing and controlling charging effects. It is not a NASA or Air Force mandatory requirement unless specifically included in project specifications. It is expected, however, that this document, revised as experience may indicate, will provide uniform design practices for all space vehicles.

The guidelines have been compiled from published information by the NASA Lewis Research Center and the California Institute of Technology, Jet Propulsion Laboratory. Comments concerning the technical content of this document should be addressed to C. K. Purvis at the NASA Lewis Research Center.

Some of the information contained in this document was assembled under contract NAS3-21048 by Robert E. Kamen and Alan B. Holman, SAI Incorporated. Significant contributions to that effort were made by Edward O'Donnell, Michael Grajek, Rita Simas, and Donald McPherson, SAI Incorporated. Special appreciation is extended to the following companies and agencies for the information they supplied for this document: Air Force Materials Laboratory, Beers Associates, Communication Spacecraft Corporation, Ford Aerospace, General Electric, Hughes Aircraft, IRT Corporation, NASA Goddard Space Flight Center, Naval Research Laboratory, Mission Research Corporation, Rockwell-International, and the Air Force Space Division. K. Duff and D. Hoshino prepared the manuscript and G. Plamp provided data on material properties.

Contents

1.0 Introduction

These guidelines are intended to provide a ready reference for spacecraft systems designers and others needing an overall view of the techniques required to limit the detrimental effects of spacecraft charging. The primary goals of this document are to summarize the available information on controlling charging effects and to provide guidelines for incorporating immunity to electromagnetic transients into spacecraft and spacecraft subsystems.

1.1 Definition of Spacecraft Charging

Spacecraft charging is defined as those phenomena associated with the buildup of charge on exposed external surfaces of geosynchronous spacecraft. This surface charging results from spacecraft encounter with a geomagnetic substorm environment—a plasma with particle energies from 1 to 50 keV.

Two types of spacecraft charging will be considered. The first, called absolute charging, occurs when the entire spacecraft potential relative to the ambient space plasma is changed uniformly by the encounter with the charging environment. The second type, called differential charging, occurs when parts of the spacecraft are charged to different negative potentials relative to each other. In this type of charging, strong local electric fields may exist.

1.2 Spacecraft Charging Concerns

The designer must recognize the importance of mission role and spacecraft configuration in evaluating absolute and differential charging effects. The buildup of large potentials on spacecraft relative to the ambient plasma is not, of itself, a serious electrostatic discharge (ESD) design concern. However, such charging enhances surface contamination, which degrades thermal properties. It also compromises scientific missions seeking to measure properties of the space environment. Spacecraft systems referenced to structure ground are not affected by a uniformly charged spacecraft. However, spacecraft surfaces are not uniform in their material properties, surfaces will be either shaded or sunlit, and the ambient fluxes may be anisotropic. These and other charging effects can produce potential differences between spacecraft surfaces or between spacecraft surfaces and spacecraft ground. When a breakdown threshold is exceeded, an electrostatic discharge can occur. The transient generated by this discharge can couple into the spacecraft electronics and cause upsets ranging from logic switching to complete system failure. Discharges can also cause long-term degradation of exterior surface coatings and enhance contamination of surfaces. Vehicle torquing or wobble can also be produced when multiple discharges occur. The ultimate results are disruptions in spacecraft operation.

1.3 Initial Environmental Considerations

1.3.1 Environment

The nature of the space environment and the role it plays will be explained in some detail later. As an introduction, and for those who may not care to involve themselves in analytic details, key concepts are presented here.

The composition and time evolution of the space plasma environment are quite complex (see, e.g. DeForest, 1971; and Garrett, Pavel, and Hardy, 1977). It is standard practice to represent the environment in terms of a temperature and density, assuming a Maxwell-Boltzmann distribution. In that characterization the geosynchronous environment is typified as a cold, dense plasma (with a "temperature" of about 1 eV and a density of 100 particles/cm^3). During a geomagnetic substorm the high-density, low-energy plasma near local midnight is replaced by a cloud of low-density plasma (1 to 10 particles/cm^3) with energies from 1 to 50 keV. It is this environment that can charge spacecraft dielectric surfaces to the extent that they may break down in an electrostatic discharge. The hot plasma cloud diffuses in a few hours but is replaced many times during the life of the storm (which may last a day or longer). For persons choosing to do analytical work, a "worst case" environment is defined in section 2.1.

If the spacecraft is near local noon when the cloud appears, it may never see the hot plasma and will not charge. If the spacecraft is near midnight, it may experience charging and upsets. If the spacecraft is near local evening, as it moves toward midnight it will pass into the diffusing cloud and a more severe charging environment. If the spacecraft is near local dawn, it may

be overtaken by the hot plasma. The problem for the spacecraft designer is that each of these environments represents a unique set of plasma conditions as viewed by the spacecraft and results in a markedly different charging history.

For absolute charging the spacecraft potential changes as a whole—the dielectric surface voltages are "locked" to the ground reference voltage. This type of charging occurs very rapidly (in fractions of a second), typically during eclipse. Differential charging usually occurs slowly (in minutes) and results in one part or surface being charged to a potential different from those of other parts of the spacecraft. This differential charging can also change the absolute charging level of the spacecraft. This is the usual mechanism for daylight charging, which consequently occurs slowly.

1.3.2 Spacecraft role

A critical factor influencing the extent to which charging interactions must be controlled is the mission of the spacecraft. In all spacecraft, differential charging is undesirable. For scientific spacecraft, absolute charging usually is not desired. For such spacecraft, conductive-coated dielectrics can be used to minimize differential surface charging, and active charge control devices can be incorporated to hold the spacecraft potential close to the space plasma potential. For operational spacecraft the effort should be directed toward controlling those charging effects that are detrimental to the particular mission.

More definitive data on environmentally induced effects in geosynchronous satellites are needed. This data base could be obtained if all such spacecraft carried environment and event monitors (section 5.2).

1.3.3 Spacecraft configuration

Also of major concern in determining the importance of spacecraft charging is the effect of spacecraft configuration on charging behavior. A spin-stabilized spacecraft usually has a low spacecraft ground potential (a few hundred volts negative). On some shaded dielectric surfaces during sunlit charging events, differential voltages of several thousand volts can occur.

A three-axis-stabilized spacecraft can have a rather large negative structure potential (a few thousand volts) in sunlit charging events. The dominant areas controlling charging in this case are the backs of the solar array wings. Differential charging will likely not be as large as in the spinner case (Purvis, 1980).

1.3.4 Effect of charging on systems

The geosynchronous substorm environment will charge spacecraft exterior surfaces. Since different materials are used and since sunlight can illuminate only one side at a time, there will always be some differential charging as well as absolute charging. The effect of this surface charging on the performance of spacecraft must be evaluated in terms of malfunctions, upsets, and failures.

As stated, surface charging could disrupt environmental measurements on scientific spacecraft. For this application and others where control of electrostatic fields is required, material selection to minimize differential charging is mandatory. For operational spacecraft, surface charging can also cause problems. The hallmark of the spacecraft charging phenomenon is the occurrence of electronic switching anomalies. These anomalies are believed to result from transients caused by differential-charging-induced discharges. These anomalous events even seem to occur in systems that are supposedly immune to noise. The discharge-induced transients, under very severe environmental conditions, can cause system failures.

Surface charging also enhances contamination. The contaminants are attracted back to charged surfaces and deposit on them. This changes surface characteristics. Altered surface optical properties result in higher temperatures. Changes in secondary and photoelectron yields result in altered charging characteristics. Deposition of dielectric contaminants can also reduce surface conductivity. If there are severe discharges on the surfaces, the materials can be damaged and can change the thermal control performance.

1.4 Design Guidelines Format

This document has been prepared as a guide to spacecraft system designers. These guidelines should be used early in the design process so that the control of spacecraft charging can be easily and economically achieved. It should be stressed that, if such control is to be successfully incorporated, care must be exercised throughout the program to ensure compliance with the guidelines. Each spacecraft is different, and these generalized guidelines must be adapted and modified to fit the particular application.

The document is divided into five parts. The first section has introduced spacecraft charging concepts of importance to the designer. The following section details the modeling techniques to be used to assess whether the design is adequate for environmental immunity. The third section presents specific guidelines for protecting systems and subsystems. This is followed by a section describing test procedures for demonstrating system immunity. The fifth section discusses active charge control and monitoring techniques. Appendixes present illustrative examples and the bibliography lists other documents for those desiring further information on specific topics.

2.0 Spacecraft Modeling Techniques

Modeling is an essential activity in spacecraft design and in evaluating spacecraft charging effects. There are four regimes of interest in modeling these effects. First, the ambient environment and its fluctuations must be specified. Second, the interaction process—the buildup of charge and electric fields near the vehicle—must be modeled. Third, given the existence of charged surfaces and potential gradients, the likelihood, signal characteristics, and frequency of electrostatic discharge must be modeled. Finally, the coupling of the electrostatic discharge pulse to individual circuit elements must be modeled in order to identify the spacecraft elements most likely to be affected. Recommended modeling procedures are presented in this section along with overviews of the physical processes involved.

For brevity in the discussion that follows, some of the more detailed material has been placed in the appendixes.

2.1 Substorm Environment Specifications

Worst-case environments should be used in predicting spacecraft potentials. The ambient space plasma and the solar extreme ultraviolet (EUV) are the major sources of spacecraft charging currents in the natural environment. The ambient space plasma consists of electrons, protons, and other ions. All of the particles have energies, which are often described by the "temperature" of the plasma. A spacecraft in this environment will accumulate charges until an equilibrium is reached in which the net current is zero. The net current to a surface is the sum of currents due to ambient electrons and ions, secondary electrons, and photoelectrons. The EUV-created photoelectron emissions usually dominate in geosynchronous orbits and prevent the spacecraft potential from being very negative during sunlit portions of the mission.

The density of the plasma also affects spacecraft charging. A "thin," or tenuous, plasma of less than 1 particle/cm^3 will charge the spacecraft and its surfaces more slowly than a "dense" plasma of thousands of particles per cubic centimeter. Also the thin plasma's current can be leaked off partially dielectric surfaces, and steady-state surface and potential differences may not be as great as those in a dense plasma.

Although the photoelectron current due to solar EUV dominates over most of the magnetosphere, in and near geosynchronous orbit during geomagnetic substorms the ambient hot electron current can control and dominate the charging process. Unfortunately the ambient plasma environment at geosynchronous orbit is very difficult to describe. To simplify this description for design purposes, typically only the isotropic currents and Maxwellian temperatures are presented—and these only for the electrons and protons. Useful answers can be obtained with this simple representation. For a worst-case static charging analysis the "single Maxwellian" environmental characterization given in table I is recommended.

The values given in table I are a 90th percentile single-Maxwellian representation of the environment (appendix A). Section 2.3 describes the spacecraft charging equations and methods in which these values will be used to predict spacecraft charging effects. If the worst-case analysis shows that spacecraft surface differential potentials are less than 500 V, there should be no electrostatic discharging problem. If the worst-case analysis shows a possible problem, use of more realistic plasma parameters should be considered.

A more comprehensive discussion of plasma parameters is given in appendix A. Some original data are presented for the ATS-5, ATS-6, and SCATHA satellites, with average values, standard deviations, and worst-case values. Additionally, percentages of yearly occurrences are given, and finally, a typical time history of a model substorm is shown. All of these different descriptions of plasma parameters can be used to help analyze special or extreme spacecraft charging situations.

2.2 Spacecraft Surface Charging Models

Analytical modeling techniques should be used to predict surface charging effects. In this section, approaches to predicting spacecraft surface voltages resulting from encounters with the substorm environment are discussed. The predictions identify possible discharge locations and are used to establish the spacecraft and component level test requirements.

2.2.1 Simple approximations

The simple approximations discussed in this section are of a worst-case nature. If this analysis indicates differential potentials of less than 500 V, there should be no spacecraft discharge problems. If predicted potentials on materials exceed 500 V, the NASA Charging Analyzer Program (NASCAP) code (section 2.2.2) must be used.

Although the physics behind the spacecraft charging process is quite complex, the formulation at geosynchronous orbit can be expressed in very simple terms if a

TABLE I. - WORST-CASE GEOSYNCHRONOUS PLASMA ENVIRONMENT

Electron number density, N_E, cm^{-3}	1.12
Electron temperature, T_E, eV	1.2×10^4
Ion number density, N_I, cm^{-3}	2.36×10^{-1}
Ion temperature, T_I, eV	2.95×10^4

Maxwell-Boltzmann distribution is assumed. The fundamental physical process for all spacecraft charging is that of current balance—at equilibrium, all currents must sum to zero. The potential at which equilibrium is achieved is the potential difference between the spacecraft and the space plasma ground. The basic equation expressing this current balance for a given surface in an equilibrium situation is, in terms of the current:

$$I_E(V) - [I_I(V) + I_{SE}(V) + I_{SI}(V) + I_{BSE}(V) + I_{PH}(V) + I_B(V)] = I_T \qquad (1)$$

where

V	spacecraft potential
I_E	incident electron current on spacecraft surface
I_I	incident ion current on spacecraft surface
I_{SE}	secondary electron current due to I_E
I_{SI}	secondary electron current due to I_I
I_{BSE}	backscattered electrons due to I_E
I_{PH}	photoelectron current
I_B	active current sources such as charged particle beams or ion thrusters
I_T	total current to spacecraft (at equilibrium, $I_T = 0$)

For a spherical body and a Maxwell-Boltzmann distribution, the first-order current densities (the current divided by the area over which the current is collected) can be shown (Garrett, 1981) to be given by

Electrons

$$J_E = J_{EO} \exp\left(\frac{qV}{kT_E}\right) \qquad V<0 \text{ repelled} \qquad (2)$$

$$J_E = J_{EO}\left[1 + \left(\frac{qV}{kT_E}\right)\right] \qquad V>0 \text{ attracted} \qquad (3)$$

Ions

$$J_I = J_{IO} \exp\left(-\frac{qV}{kT_I}\right) \qquad V>0 \text{ repelled} \qquad (4)$$

$$J_I = J_{IO}\left[1 - \left(\frac{qV}{kT_I}\right)\right] \qquad V<0 \text{ attracted} \qquad (5)$$

where

$$J_{EO} = \left(\frac{qN_E}{2}\right)\left(\frac{2kT_E}{\pi m_E}\right)^{1/2}$$

and

$$J_{IO} = \left(\frac{qN_I}{2}\right)\left(\frac{2kT_I}{\pi m_I}\right)^{1/2} \qquad (6)$$

where N_E and N_I are densities of electrons and ions, respectively; m_E and m_I are masses of electrons and ions, respectively; and q is the magnitude of the electronic charge.

Given these expressions and parameterizing the secondary and backscatter emissions, equation (1) can be reduced to an analytic expression in terms of the potential at a point. This model, called an analytic probe model, can be stated as follows:

$$A_E J_{EO}[1 - SE(V, T_E, N_E) - BSE(V, T_E, N_E)] \exp\left(\frac{qV}{kT_E}\right) - A_I J_{IO}[1 + SI(V, T_I, N_I)]\left[1 - \left(\frac{qV}{kT_I}\right)\right] - A_{PH} J_{PHO} f(X_m) = I_T = 0 \qquad V<0 \qquad (7)$$

where

A_E	electron collection area
J_{EO}	ambient electron current density
A_I	ion collection area
J_{IO}	ambient ion current density
A_{PH}	photoelectron emission area
J_{PHO}	saturation photoelectron flux
BSE,SE,SI	parameterization functions for secondary emission due to backscatter, electrons, and ions
$f(X_m)$	attenuated solar flux as a function of altitude X_m of center of Sun above surface of Earth as seen by spacecraft, percent

This equation is appropriate for a small (<10 m), uniformly conducting spacecraft at geosynchronous orbit in the absence of magnetic field effects. To solve the equation, V is varied until $I_T = 0$. Typical values of SI, SE, and BSE are 3, 0.4, and 0.2, respectively, for aluminum. For geosynchronous orbit, J_E/J_I is about 30 during a geomagnetic storm. When the spacecraft is in eclipse, these values give

$$V \approx -T_E \qquad (8)$$

where T_E is in electron volts. That is, to first order in eclipse, the spacecraft potential is approximately numerically equal to the plasma temperature expressed in electron volts. Note, however, that T_E must exceed some critical value (Olsen, 1983; Garrett et al., 1979), usually of the order of 1000 eV, before charging will occur because secondary electron production can exceed ambient current for low enough T_E.

2.2.2 NASA Charging Analyzer Program (NASCAP)

The NASA Charging Analyzer Program computer code (Katz et al., 1977, 1979; Schnuelle et al., 1979; Roche and Purvis, 1979; Rubin et al., 1980) has been specifically developed as an engineering tool to determine the environmental effect on spacecraft surfaces and systems. It can analyze the surface charging of a three-dimensional, complex body as a function of time for given space environmental conditions and specified surface potentials. Material properties of surfaces are included in the computations. Surface potentials, low-energy sheath properties, potential distributions in space, and particle trajectories are computed. By locating severe surface voltage gradients in a particular design, it is possible to show where discharges could occur. The effect of changes in the surface materials or coatings in those areas on minimizing voltage gradients can then be evaluated. The environment of table I should be used in these analyses. NASCAP is described in detail in appendix B.

2.3 Discharge Characteristics

Charged spacecraft surfaces can discharge, and the resulting transients can couple into electrical systems. A spacecraft in space must be considered to be a capacitor relative to the space plasma potential. The spacecraft, in turn, is divided into numerous other capacitors by the dielectric surfaces used for thermal control and for power generation. This system of capacitors can be charged at different rates depending on incident fluxes, time constants, and spacecraft configuration effects. Because of this complex charging rate pattern, sophisticated computer programs are required to predict behavior.

The system of capacitors floats electrically with respect to the space plasma potential. This can give rise to unstable conditions in which charge can be lost from the spacecraft to space. Whether anyone will ever be able to establish exact conditions required for such breakdowns is questionable. What is known is that breakdowns do occur, and it is hoped that conditions that lead to breakdowns can be bounded.

Breakdowns, or discharges, probably occur because a differential charge builds up in spacecraft dielectric surfaces or between various surfaces on the spacecraft. Whenever this charge buildup generates an electric field that exceeds a breakdown threshold, charge will be released from the spacecraft to space. This charge release will continue until the differential driving force no longer exists. Hence, the amount of charge released will be limited to the total charge stored in or on the dielectric at the discharge site. The charge loss or current to space causes the dielectric surface voltage (at least locally) to relax toward zero. Since the dielectric is capacitively coupled to the structure, the charge loss will also cause the structure potential to become less negative. In fact, the structure could become positive with respect to the space plasma potential. The exposed conductive surfaces of the spacecraft will then collect electrons from the environment (or attract back the emitted ones) to reestablish the structure potential required by the substorm conditions. The whole process can take microseconds. Multiple discharges can be produced if substorm intensities remain high long enough to reestablish the conditions necessary for a discharge.

For a long time it was believed that there could be a charge loss over an extended area of the dielectric. This phenomenon would have produced area-dependent charge losses capable of generating currents of hundreds of amperes. This concept was based on testing of grounded substrate samples, which produced spectacular lightning-strike photographs. The differential voltages necessary to produce this large charge-cleanoff type of discharge were typically in excess of 10 kV. Since spacecraft modeling and current spaceflight data indicate differential voltages of only 3 to 4 kV, it must be assumed that actual discharges are much milder and limited in charge loss. Without the strong differential voltages on the dielectrics, the large-area charge cleanoff probably will not occur.

Since breakdowns are believed to be due to differential charging, they can occur during sunlit charging events. Because sunlight tends to keep all illuminated surfaces near plasma potential, whereas shaded dielectric surfaces may charge strongly negatively, sunlight enhances differential charging. Entering and exiting eclipse, in contrast, result in a change in absolute charging for all surfaces except those weakly capacitively coupled to the structure (capacitance to structure less than that of spacecraft to space, normally $<2\times10^{-10}$ F). Differential charging in eclipse develops slowly and depends on differences in secondary yield. In the following paragraphs each of the identified breakdown mechanisms is summarized.

2.3.1 Dielectric surface breakdowns

If either of the following criteria are exceeded, discharges can occur:

(1) Dielectric surface voltages are greater than 500 V positive relative to an adjacent exposed conductor.

(2) The interface between a dielectric and an exposed conductor has an electric field greater than 1×10^{5} V/cm. Note that edges, points, gaps, seams, and imperfections in surface materials can increase electric fields and hence promote the probability of discharges. These items are not usually modeled and must be found by close inspection of the exterior surface specifications.

The first criterion can be exceeded by solar arrays in which the high secondary yield of the coverslide can result in surface voltages that are positive with respect to the metalized interconnects. This criterion can also apply

to metalized dielectrics in which the metalized film, either by accident or design, is isolated from structure ground by a resistance value greater than 10 MΩ (essentially only capacitively coupled). In the latter case, the dielectric can be charged to large negative voltages (when shaded), and the metal film will thus become more negative than the surrounding surfaces and act as a cathode or electron emitter.

The second criterion applies to those areas of a spacecraft where a strong negative voltage gradient could exist. This usually would be associated with the edge of a dielectric next to another surface or with cracks in the dielectric exposing a conductor underneath. The charge stored on or in the dielectric is relatively unstable and could be lost.

In both of these conditions, stored charge is initially ejected to space in the discharge process. This loss produces a transient that can couple into the spacecraft structure and possibly into the electronic systems. Current returns from space to the exposed conductive areas of the spacecraft. Transient currents flow in the structure depending on the electrical characteristics. It is assumed that the discharge process will continue until the voltage gradient or electric field that began the process disappears. The currents flowing in the structure will damp out according to its resistance.

The computation of charge lost in any discharge is highly speculative at this time. Basically, charge loss can be considered to result from the depletion of two capacitors: that stored in the spacecraft, which is charged to a specified voltage relative to space, and that stored in a limited region of the dielectric at the discharge site. The computation of the charge loss is a question of judgment on the part of the analyst and must depend on the predicted voltages on the spacecraft at the time that discharges are expected to occur. As a guide the following charge loss categories might be useful:

$Q_{lost} < 0.5\ \mu C$—minor discharge

$Q_{lost} < 2\ \mu C$—moderate discharge

$Q_{lost} < 10\ \mu C$—severe discharge

The current in a discharge pulse can be modeled in any of several ways, such as approximation by square, triangular, or double exponential pulses or by a resistance-inductance-capacitance (RLC) series circuit.

As an example, an RLC model yields a current given by

$$I_D = \left(\frac{V_D}{2L}\right) \exp\left(\frac{-Rt}{2L}\right) - \frac{\exp(dt) - \exp(-dt)}{d}$$

where

$$d = \left(\frac{R}{2L}\right)^2 - \left(\frac{1}{LC}\right)^{1/2}$$

The dielectric surface voltage change with time can be computed from

$$I_D = C\frac{dV_D}{dt}$$

where V_D is the value of the dielectric surface voltage at time t. By integrating this expression the charge loss can be determined. The resistance, inductance, and capacitance values can be adjusted to produce a desired charge loss simulating the estimated stored charge that is predicted in the discharge. The duration of the pulse is the time required for the current to go to zero. Typical examples of this procedure for discharge currents are shown in figure 1 for the cases where the dielectric is charged to −2000, −5000, and −10 000 V just before discharge. Figure 2 shows the associated changes in dielectric surface voltages.

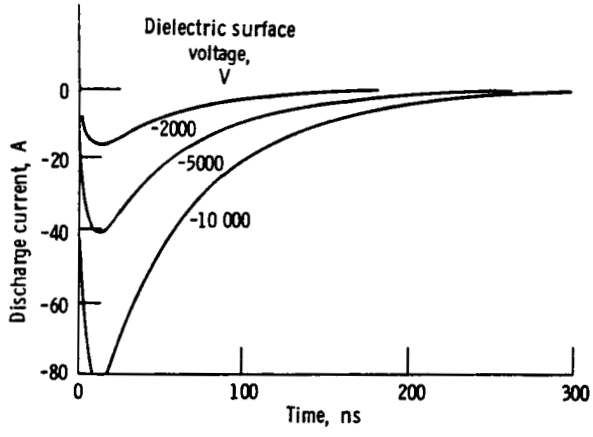

Figure 1.—Predicted discharge current transients.

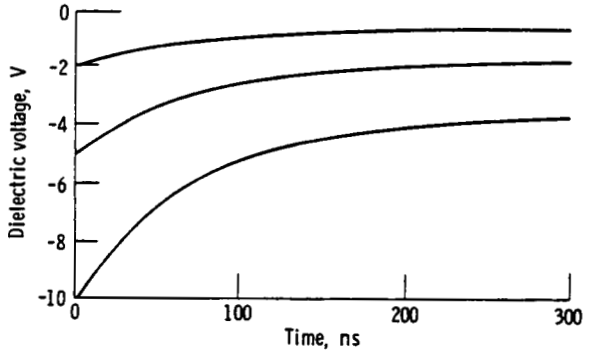

Figure 2.—Change in dielectric surface voltage due to discharges.

2.3.2 Buried charge breakdowns

This section refers to the situation where charges have sufficient energy to penetrate slightly below the surface of a dielectric and are trapped. If the dielectric surface is maintained near zero potential due to photoelectron or secondary-electron emission, strong electric fields may exist in the material.

This can lead to electric fields inside the material large enough to cause breakdowns. Breakdown can occur whenever the internal electric field exceeds 2×10^5 V/cm. As an example, figure 3 illustrates the electric fields inside a Teflon film irradiated by a 12-keV electron beam. Note that the field changes sign inside the material, at a depth of about 0.5 μm for this example. The zero field depth divides the dielectric into two regions for field buildup, labeled regions I and II in the figure. Simple models for the currents and fields in these regions can be used to obtain estimates of the conductivity required to avoid buildup of fields larger than 2×10^5 V/cm.

The differential equation relating currents and fields in each of the two regions (for a linear dielectric in one dimension) is

$$\epsilon\frac{dE(x,t)}{dt}+s(x)E(x,t)=J(x)$$

where ϵ is the dielectric constant, $s(x)$ is the conductivity at depth x, $E(x,t)$ is the electric field, and $J(x)$ is the current density. The solution to this equation, assuming $J(x)$ and $s(x)$ are independent of time, is

$$E(x,t)=E_0(x)\exp\left[\frac{s(x)t}{\epsilon}\right]-\left[\frac{J(x)}{s(x)}\right]\times\left(1-\exp\left\{1-\exp\left[\frac{-s(x)t}{\epsilon}\right]\right\}\right)$$

where $E_0(x)$ is the field at $t=0$. At long times this reduces to the form $E=J/s$. Appropriate identification of J for each region can thus be used to estimate s values.

The J for each region can be identified by considering the equivalent circuit diagram of figure 4. Here the node labeled 0 represents the zero field point, J_F is the current from the front to space, and J_B that to spacecraft ground (assumed equivalent to plasma ground). In region I the strongest electric fields are near the substrate, and the appropriate conductivity is that for the unirradiated dielectric material. The current in this region can be as much as 33 percent of the injected current. Substorm current densities are typically in the range 0.1 to 1.0 nA/cm^2, giving a value of $\sim$0.3 nA/cm^2 for J_B. This yields an estimate of $s\sim1.5\times10^{-15}$ mho/cm for the minimum allowable dark conductivity.

In region II the largest electric fields will develop near the front surface. In this region the conductivity includes radiation-induced terms and is generally higher than the dark conductivity. However, because the currents are also larger, strong fields can develop. The maximum field is $J_F/s(x=0)$, where J_F can range from a small initial value to a large fraction of the incoming current density. This yields $s\sim5\times10^{-15}$ mho/cm for the minimum total conductivity.

Note that the form of the internal electric field is determined by the spectrum of the incoming electrons, so that the conductivity guidelines derived here are approximate. Better estimates of the field under particular circumstances should be used if available.

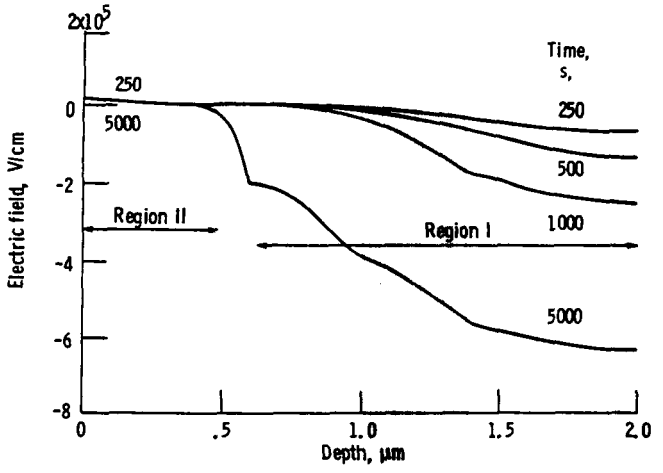

Figure 3.—Evolution of electric field with time in 0.13-mm (5-mil) Teflon. Calculated for 12-keV monoenergetic electron beam at 0.1 nA/cm^2.

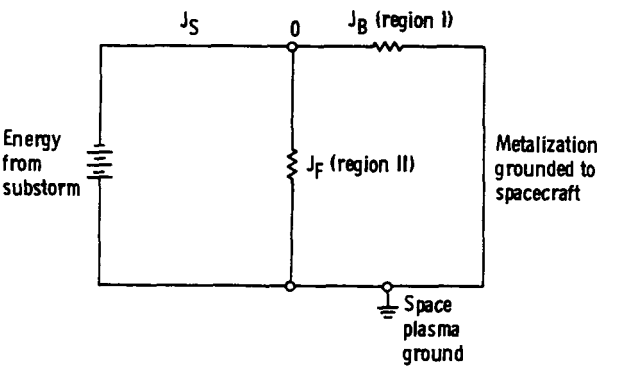

Figure 4.—Circuit with which to estimate internal electric fields.

2.3.3 Spacecraft-to-space breakdowns

Spacecraft-to-space breakdowns are generally similar to dielectric surface breakdowns but involve only small discharges. It is assumed that a strong electric field exists on the spacecraft surfaces—usually due to a geometric interfacing of metals and dielectrics. This arrangement periodically triggers a breakdown of the spacecraft-to-space capacitor. Since this capacitance tends to be of the order of 2×10^{-10} F, these breakdown transients should be small and rapid.

2.4 Coupling Models

Coupling model analyses must be used to determine the hazard to electronic systems from exterior discharge transients. In this section, techniques for computing the influence of exterior discharge transients on interior spacecraft systems are discussed.

2.4.1 Lumped-element modeling

Lumped-element models (LEM) have been used to define the surface charging response to environmental fluxes (Robinson and Holman, 1977; Inouye, 1976; Massaro et al., 1977; Massaro and Ling, 1979) and are currently used to predict interior structural currents resulting from surface discharges. The basic philosophy of a lumped-element model is that spacecraft surfaces and structures can be treated as electrical circuit elements—resistance, inductance, and capacitance. The geometry of the spacecraft is considered only to group or lump areas into nodes within the electrical circuit in much the same way as surfaces are treated as nodes in thermal modeling. Therefore, these models can be made as simple or as complex as is considered necessary for the circumstances.

LEM's developed to predict surface charging rely on the use of current input terms applied independently to surfaces. Since there are no terms relating the influence of charging by one area on the incoming flux to other areas, the predictions usually result in larger negative voltages than actually observed. Other modeling techniques, such as NASCAP, more realistically treat these three-dimensional effects and predict surface voltages closer to those measured.

The LEM's for discharges assume that the structure current transient is generated by capacitive coupling to the discharge site and is transmitted in the structure by conduction only. An analog circuit network is constructed by taking into consideration the structure properties and the geometry. This network must consider the principal current flow paths from the discharge site to exposed conductor areas—the return path to space plasma ground. Discharge transients are initiated at regions in this network selected as being probable discharge sites by surface charging predictions or other means. Transient characteristics are controlled by choosing values of resistance, capacitance, and inductance to space. The resulting transients within the network can be solved by using network computer transient circuit analysis programs such as ISPICE or SPICE2.

The procedure is illustrated in the following simplified example. Consider a three-axis-stabilized spacecraft (fig. 5) with a shaded dielectric area adjacent to a conductor. The spacecraft is charged by a substorm such that the structure potential is about -2.5 kV while the shaded dielectric is at about -5900 V. These values were obtained from NASCAP runs. Figure 6 shows one section of that spacecraft where a discharge could occur. According to the breakdown criteria given in section 2.3.1, a discharge should occur that would eject ~ 3 μC of charge in about 0.15 μs.

A very simplified, single-path lumped-element model to simulate the discharge conditions in a spacecraft is shown in figure 7. It is assumed that the spacecraft is charged relative to the space plasma potential by a substorm environment. The spacecraft and dielectric are differentially charged to -2500 and -5000 V, respectively, at which time a discharge occurs. The discharge model assumes that the discharge time is short compared with the charging times—when switch S1 closes, S2 is assumed to open. The discharge-pulse-shaping network allows whatever charge is assumed to be stored in the dielectric to leave in a controlled fashion (fig. 1). The transient caused by the discharge is capacitively coupled into the structure. The single-path representation of the structure is modeled as a resistor, capacitor, and inductor chosen to produce an underdamped oscillation with a frequency of about 10 MHz—the estimated value of the structure resonance.

The discharge results in the dielectric surface voltage becoming more positive. This forces the spacecraft voltage (relative to space) also to become more positive. Eventually, the spacecraft must return to its substorm-driven value, and this can be estimated by assuming that the vehicle is a capacitor being recharged with a given time constant (fig. 8(a)). Here, the spacecraft potential rises for 200 ns, at which time it returns rapidly to its original value of -2500 V.

The current induced in the structure by this discharge is shown in figure 8(b). The first 200 ns corresponds to the response to the discharge. The flatter region at 200 ns corresponds to the period in which the structure is recharging. The oscillations beyond 200 ns are the ringing current at the structure frequency. This ringing is damped out by the structure resistance. It should be stressed that this is an extremely simplified model used to explain a complex interaction. In reality, there would be many paths for current flows from the essentially point source of a discharge throughout the structure back to space. This produces complex wave patterns in the structure that

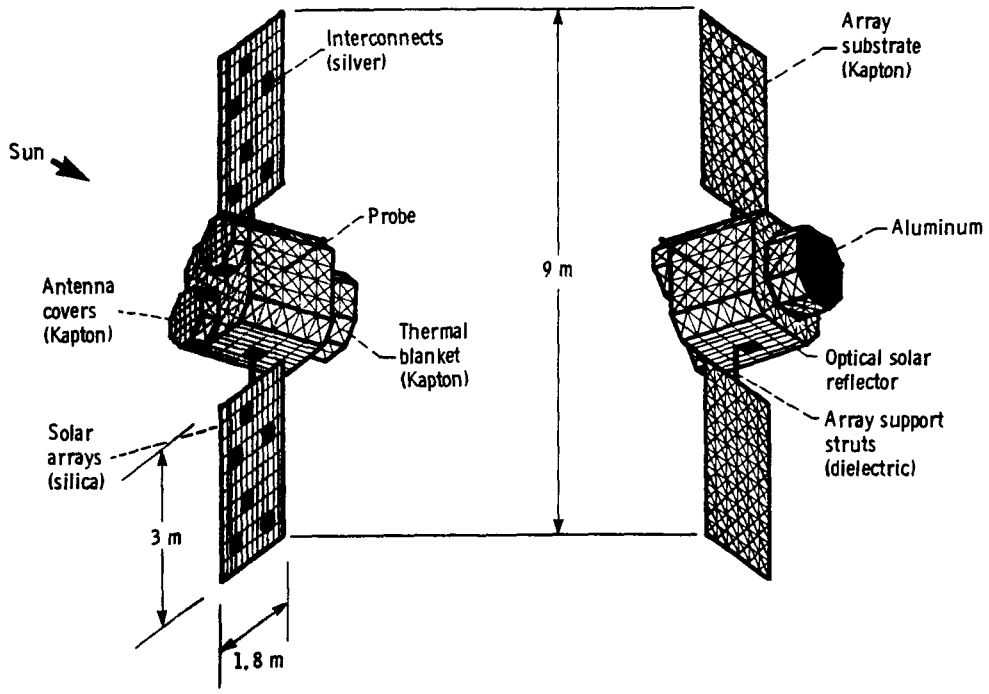

Figure 5.—Three-axis-stabilized geosynchronous satellite.

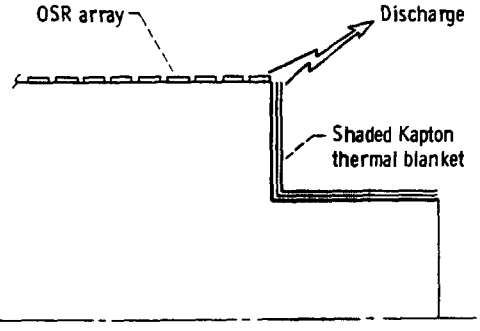

Figure 6.—External surface discharge modeling—spacecraft model.

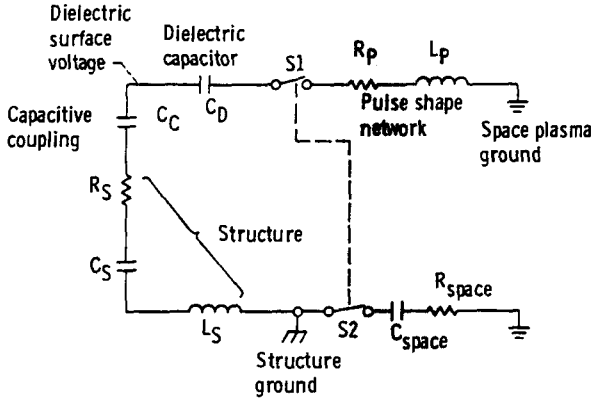

Figure 7.—External surface discharge modeling—lumped-element model.

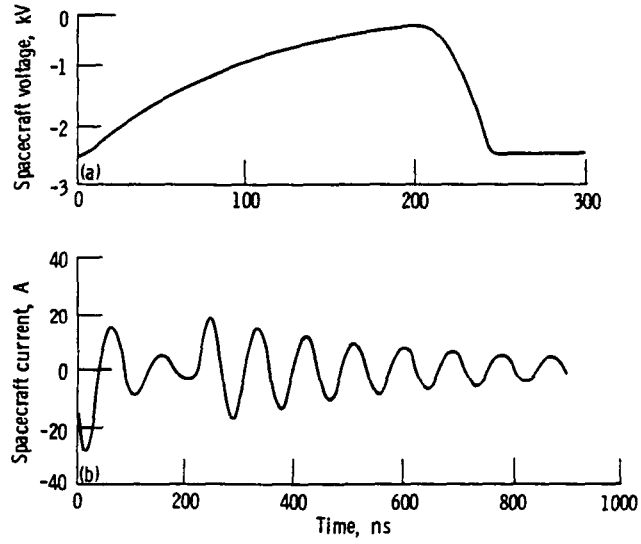

(a) Predicted change in spacecraft voltage due to discharge.
(b) Current induced in structure by discharge.

Figure 8.—Spacecraft response to discharge transient.

are difficult to follow. On the other hand, the simple model generates the generalized pattern but implies far larger currents than actual, where the total current flows through the single circuit. For a real case the complete analysis must be conducted.

The changing current in the structure generates a changing magnetic field, which induces a voltage in an adjacent cable or unit. This is illustrated in figure 9 along with the equivalent electrical circuit. The voltage generated in a short cable by the structure current is shown in figure 10. The oscillating pattern is distorted while the discharge is under way but changes to a damped ringing pattern afterward. The results illustrate that voltages induced in cables can be significant and can persist after the discharge session. Given the voltage and the electronic impedance, it is possible to evaluate whether a unit would be susceptible to transient upsets.

2.4.2 Specification and Electromagnetic Compatibility Program (SEMCAP)

Numerous programs have been developed to study the effects of electromagnetic coupling on circuits. Such programs have been used to compute the effects of an electromagnetic pulse (EMP) and that of an arc discharge. One program, the Specification and Electromagnetic Compatibility Program (SEMCAP) developed by TRW Incorporated (e.g., SEMCAP Program Description, Ver. 7.4, 1975, Heidebrecht), has successfully analyzed the effects of arc discharges on actual spacecraft—the Voyager series.

SEMCAP was originated to calculate cross coupling from source circuits to other circuits in a spacecraft. Arc discharges were modeled in a manner compatible with the SEMCAP input requirements, and the effects on numerous spacecraft circuits were estimated. That process is described more fully below.

Briefly, SEMCAP permits modeling the interbox harness cabling and the input and output interfaces for each box on a spacecraft. The interaction of signals on a given wire with those on every other wire is computed in terms of the physical configuration and terminating impedances. By using integration in the frequency domain over the bandwidths of the coupling networks and the receptor circuits, SEMCAP computes the peak voltage at each receptor due to each source. The designer can then compare this predicted peak voltage from each source to the threshold of susceptibility or damage of the receptor. This process identifies the most troublesome sources and the most susceptible receptors. Seeing these results suggests where to modify spacecraft design, if necessary.

Roughly 240 generators and 240 receptors can be modeled by SEMCAP. The SEMCAP code for arc discharges allows

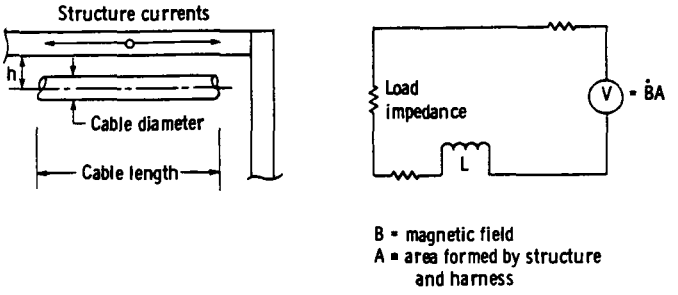

Figure 9.—Lumped-element model for cable coupling computation. (Assume $h >$ cable radius. Structure current generates magnetic field that induces voltage in cable; cable responds with its electrical characteristics.)

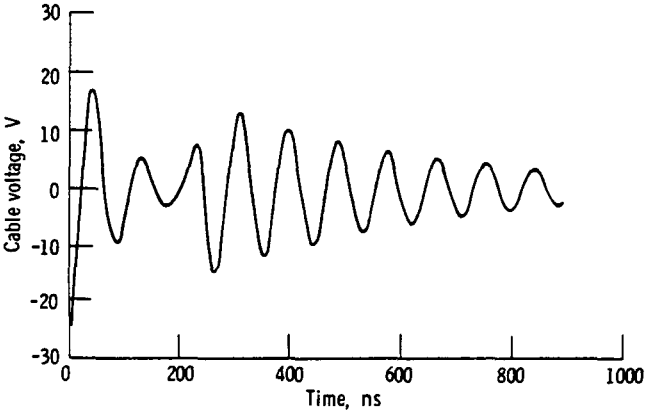

Figure 10.—Voltage generated in cable due to structure currents.

(1) Selection of diagnostic points and stimulus location

(2) Prediction of spacecraft circuit responses to test stimuli

(3) Limitation of test stimuli to benign levels

(4) Extrapolation of test responses to those expected at other locations

(5) Prediction of spacecraft responses to in-flight arcs

For illustration, the SEMCAP analysis done for Voyager is described in appendix C.

3.0 Spacecraft Design Guidelines

This section contains recommendations on design techniques that should be followed in hardening spacecraft systems to spacecraft charging effects. To minimize repetition and to make recommendations as brief as possible, this section is divided into two parts: guidelines

that are generally applicable, and ideas and comments that are more applicable to a particular subsystem, such as the power subsystem. It is suggested that all readers review the general guidelines section and read component and subsystem sections for areas of specific concern.

3.1 General Guidelines

3.1.1 Grounding

All conducting elements, surface and interior, should be tied to a common electrical ground, either directly or through a charge bleedoff resistor.

3.1.1.1 Structure and mechanical parts.—All structural and mechanical parts, electronics boxes, enclosures, etc., of the spacecraft shall be electrically bonded to each other. All principal structural elements shall be bonded by methods that assure a direct-current (dc) resistance of less than 2.5 mΩ at each joint. The collection of electrically bonded structural elements is referred to as "structure" or structure ground. The objective is to provide a low-impedance path for any ESD-caused currents that may occur and to provide an excellent ground for all other parts of the spacecraft needing grounding. If structure ground must be carried across an articulating joint or hinge, a ground strap, as short as possible, shall carry the ground across the joint. Relying on bearings to serve as a ground path is unacceptable. If structural ground must be carried across sliprings on a rotating joint, at least two, and preferably more, sliprings shall be dedicated to the structural ground path, some at each end of the slipring set. The bond to structure shall be achieved within 15 cm of the slipring on each end of the rotating joint. Sliprings chosen for grounding should be away from any sliprings carrying sensitive signals.

3.1.1.2 Surface materials.—All spacecraft surface (visible, exterior) materials should be conductive in an ESD sense (section 3.1.2). All such surface materials shall be electrically bonded (grounded) to the spacecraft structure. Because they are intended to drain space charging currents only, the bonding requirements are less severe than those for structural bonding. The dc impedance to structure should be compatible with the surface resistivity requirements: that is, less than about 10^9 Ω from a surface to structure. The dc impedance must remain less than 10^9 Ω over the service life of the bond in vacuum, under temperature, under mechanical stress, etc.

3.1.1.3 Wiring and cable shields.—All wiring and cabling exiting the shielded "Faraday cage" portion of the spacecraft (section 3.1.3) should be shielded. Those cable shields and any other cable shields used for ESD purposes shall be bonded to the Faraday cage at the entry to the shielded region as follows:

(1) The shield shall be terminated 360° around a metal shielded backshell, which is in turn terminated to the chassis 360° around the cabling.

(2) The shield ground shall not be terminated by using a pin that penetrates the Faraday cage and receives its ground inside the shielded region.

(3) A mechanism shall be devised that automatically bonds the shield to the enclosure/structure ground at the connector location, or a ground lug that uses less than 15 cm of ground wire shall be provided for the shield and procedures that verify that the shield is grounded at each connector mating shall be established.

The other end of the cable shield shall be terminated in the same manner. The goal is to maintain shielding integrity even when some electronics units must be located outside the basic shielded region of the spacecraft.

3.1.1.4 Electrical and electronic grounds.—Signal and power grounds require special attention in the way they are connected to the spacecraft structure ground. For ESD purposes a direct wiring of all electrical/electronics units to structure is most desirable. In particular, one should not have separate ground wires from unit to unit or from each unit to a single point on the structure.

If the electronic circuitry cannot be isolated from power ground, signal ground may be referenced to structure with a large (> 10 kΩ) resistor. Once again, box-to-box signals must be isolated to prevent ground loops. This approach must be analyzed to assure that it is acceptable from an ESD standpoint.

In some cases it is necessary to run signal and power ground lines in harnesses with other space vehicle wiring. This should be avoided where possible and limited where considered necessary. Excessively long runs of signal ground lines should be eliminated.

3.1.2 Exterior surface materials

For differential charging control, all spacecraft exterior surfaces shall be at least partially conductive. The best way to avoid differential charging of spacecraft surfaces is to make all surfaces conductive and grounded

to the spacecraft structure. However, typical spacecraft surface materials often include insulating films such as Mylar, Kapton, Teflon, fiberglass, glass, quartz, or other dielectric materials. It should be recognized in the design phase that there may be areas for which use of conductive surfaces is particularly crucial, such as areas adjacent to receivers/antennas operating at less than 1 GHz, sensitive detectors (Sun and Earth detectors, etc.) or areas where material contamination or thermal control is critical. For these applications use of indium tin oxide (ITO) coatings is recommended.

This section first defines the conductivity requirements for spacecraft surface materials. Materials that are typically used are then evaluated and their usage is discussed. Analysis is suggested to estimate the effects of any dielectric surfaces that may remain on the spacecraft. At the conclusion of this section, use of materials with a high secondary electron yield is discussed.

3.1.2.1 Surface conductivity requirements.—To discharge surfaces that are being charged by space plasmas, a high resistivity to ground can be tolerated because the plasma charging currents are small. The following guidelines are recommended:

(1) Conductive materials (e.g., metals) must be grounded to structure with the smallest resistance possible

$$R < 10^9/A, \ \Omega$$

where A is the exposed surface area of the conductor in square centimeters.

(2) Partially conductive surfaces (e.g., paints) applied over a conductive substrate must have a resistivity-thickness product

$$rt \leq 2 \times 10^9, \ \Omega\text{-cm}^2$$

where r is the material resistivity in ohm-centimeters and t is the material thickness in centimeters.

(3) Partially conductive surfaces applied over a dielectric and grounded at the edges must have material resistivity such that

$$\frac{rh^2}{t} \leq 4 \times 10^9, \ \Omega\text{-cm}^2$$

where r and t are as above and h is the greatest distance on a surface to a ground point, in centimeters.

These guidelines depend on the particular geometry and application. A simplified set of guidelines is supplied for early design activities:

(1) Isolated conductors must be grounded with less than 10^6 Ω to structure.

(2) Materials applied over a conductive substrate must have bulk resistivities of less than 10^{11} Ω-cm.

(3) Materials applied over a dielectric area must be grounded at the edges and must have a resistivity less than 10^9 "ohms per square."[1]

These requirements are more strict than the preceding relations, which include effects of spacecraft geometry.

In all cases the usage or application process must be verified by measuring resistance from any point on the material surface to structure. Problems can occur. For example, one case was observed where a nonconductive primer was applied underneath a conductive paint; the paint's conductivity was useless over the insulating primer.

All grounding methods must be demonstrated to be acceptable over the service life of the spacecraft. It is recommended that all joint resistances and surface resistivities be measured to verify compliance with these guidelines. Test voltages should be at least 500 V. Grounding methods must be able to handle current bleedoff from ESD events, vacuum exposure, thermal expansion and contraction, etc. As an example, painting around a zero-radius edge or at a seam between two dissimilar materials could lead to cracking and a loss of electrical continuity at that location.

3.1.2.2 Surface materials.—By the proper choice of available materials the differential charging of spacecraft surfaces can be minimized. At present, the only proven way to eliminate spacecraft potential variations is by making all surfaces conductive and tying them to a common ground.

Surface coatings in use for this purpose include conductive conversion coatings on metals, conductive paints, and transparent partially metallic vacuum-deposited films, such as indium tin oxide. Table II describes some of the more common acceptable surface coatings and materials with a successful use history. Table III describes other common surface coatings and materials that should be avoided if possible.

The following materials have been used to provide conducting surfaces on the spacecraft:

[1] "Ohms per square" is defined as the resistance of a flat sheet of the material measured from one edge of a square section to the opposite edge. It can be seen that the size of the square has no effect on the numeric value.

TABLE II. - SURFACE COATINGS AND MATERIALS ACCEPTABLE FOR SPACECRAFT USE

Material	Comments
Paint (carbon black)	Work with manufacturer to obtain paint that satisfies ESD conductivity requirements of section 3.1.2 and thermal, adhesion, and other needs
GSFC NS43[a] paint (yellow)	Has been used in some applications where surface potentials are not a problem (apparently will not discharge)
Indium tin oxide (250 nm)	Can be used where some degree of transparency is needed; must be properly grounded; for use on solar cells, optical solar relectors, and Kapton
Zinc ortho-titanate paint (white)	Possibly the most conductive white paint; adhesion difficult without careful attention to application procedures
Alodyne	Conductive conversion coatings of magnesium, aluminum, etc., are acceptable

[a]GSFC denotes Goddard Space Flight Center.

TABLE III. - SURFACE COATINGS AND MATERIALS TO BE AVOIDED FOR SPACECRAFT USE

Material	Comments
Anodyze	Anodyzing produces a high-resistivity surface; to be avoided. The surface is thin and might be acceptable if analysis shows stored energy is small
Fiberglass material	Resistivity is too high
Paint (white)	In general, unless a white paint is measured to be acceptable, it is unacceptable
Mylar (uncoated)	Resistivity is too high
Teflon (uncoated)	Resistivity is too high. Teflon has a demonstrated long-time charge storage ability and causes catastrophic discharges
Kapton (uncoated)	Generally unacceptable, due to high resistivity. However, in continuous-sunlight applications if less than 0.13 mm (5 mils) thick, Kapton is sufficiently photoconductive for use
Silica cloth	Has been used as antenna radome. It is a dielectric, but because of numerous fibers, or if used with embedded conductive materials, ESD sparks may be individually small
Quartz and glass surfaces	It is recognized that solar cell coverslides and second-surface mirrors have no substitutes that are ESD acceptable. Their use must be analyzed and ESD tests performed to determine their effect on neighboring electronics

(1) Vacuum-metalized dielectric materials in the form of sheets, strips, or tiles. The metal-on-substrate combinations include aluminum, gold, silver, and Inconel on Kapton, Teflon, Mylar, and fused silica.

(2) Thin, conductive front-surface coatings, especially indium tin oxide on fused silica, Kapton, Teflon, or dielectric stacks

(3) Conductive paints, fog (thin paint coating), carbon-filled Teflon, or carbon-filled polyester on Kapton (Sheldahl black Kapton)

(4) Conductive adhesives

(5) Exposed conductive facesheet materials (graphite/epoxy or metal)

(6) Etched metal grids or bonded (or heat embedded) metal meshes on nonconductive substrates

(7) Aluminum foil or metalized plastic film tapes

Because of the variety in the configuration and properties of these materials, there is a corresponding variety in the applicable grounding techniques and specific concerns that must be addressed to insure reliable in-flight performance.

The following practices have been found useful:

(1) Conductive adhesives should be used to bond fused silica, Kapton, and Teflon second-surface mirrors to conductive substrates that are grounded to structure. If the substrate is not conductive, metal foil or wire ground links should be laminated in the adhesive and bolted to structure. Only optical solar reflectors (OSR's) with conductive (Inconel) back surfaces should be used.

(2) When conductive adhesives are used, the long-term stability of the materials system must be verified, particularly conductivity in vacuum after thermal cycling, compatibility of the materials (especially for epoxy adhesive) in differential thermal expansion, and long-term resistance to galvanic corrosion.

(3) Metalized Teflon is particularly susceptible to electrostatic discharge degradation, even when grounded. Avoid using it. If there is no substitute for a specific application, the effects of electromagnetic interference (EMI), contamination, and optical and mechanical degradation must be evaluated.

(4) Paints should be applied to grounded, conductive substrates. If this is not possible, their coverage should be extended to overlap grounded conductors.

(5) Ground tabs must be provided for free-standing (not bonded down) dielectric films with conductive surfaces.

(6) Meshes that are simply stretched over dielectric surfaces are not effective; they must be bonded or heat sealed in a manner that will not degrade or contaminate the surface.

(7) There are several techniques for grounding thin, conductive front-surface coatings such as indium tin oxide, but the methods are costly and have questionable reliability. The methods include welding of ground wires to front-surface metal welding contacts, front-surface bonding of coiled ground wires (to allow for differential thermal expansion) by using a conductive adhesive, and chamfering the edges of OSR's before ITO coating to permit contact between the coating and the conductive adhesive used to bond the OSR to its substrate.

Grounding techniques for OSR's include chamfering edges and bonding with conductive adhesive and front-surface bonding or welding of ground wires. Bonding down solar cell covers with conductive adhesive is not applicable. For multilayer insulation (MLI), extending the aluminum foil tab to the front surface is suitable.

3.1.2.3 Nonconductive surfaces.—If the spacecraft surface cannot be made 100 percent conductive, an analysis must be performed to show that the design is acceptable from an ESD standpoint. Note that not all dielectric materials have the same charging or ESD characteristics. The choice of dielectric materials can significantly affect surface voltage profiles. For example, it has been shown (Bever, 1981) that cerium-doped microsheet charges to much lower potentials under electron irradiation than fused silica, and it therefore may be preferred as a solar array coverslide material.

An adequate analysis preceding the selection of materials must include spacecraft analysis to determine surface potentials and voltage gradients, spark discharge parameters (amplitude, duration, frequency content), and EMI coupling. The cost and weight involved in providing adequate protection (by shielding and electrical redesign) could tilt the balance of the trade-off to favor the selection of the newer, seemingly less reliable (optically) charge control materials that are more reliable from spacecraft charging, discharging, and electromagnetic interference points of view.

The "proven" materials have their own cost, weight, availability, variability, and fabrication effects. In addition, uncertainties relating to spacecraft charging effects must be given adequate consideration. Flight data have shown apparent optical degradation of standard, stable thermal control materials (e.g., optical solar reflectors and Teflon second-surface mirrors) that is far in excess of ground test predictions, part of which could be the result of charge-enhanced attraction of charged contaminants. In addition, certain spacecraft anomalies and failures may have been reduced or avoided by using charge control materials.

Ironically, after an extensive effort to have nearly all of the spacecraft surface conductive, the remaining small patches of dielectric may charge to a greater differential potential than a larger area of dielectric would. On the shadowed side of a spacecraft, a small section of dielectric may be charged rapidly while the bulk of the spacecraft remains near zero potential because of photoemission from sunlit areas.

A spacecraft with larger portions of dielectric may have retarding electric fields because the dielectric diminishes the effects of the photoemission process. As a result, the spacecraft structure potential may go more negative and thus reduce the differential voltage between the dielectric and the spacecraft.

The lesson to be learned is that all dielectrics must be examined for their differential charging. Each dielectric region must be assessed for its breakdown voltage, its ability to store energy, and the effects it can have on neighboring electronics (disruption or damage) and surfaces (erosion or contamination).

3.1.2.4 Surface secondary emission ratios.—Other means to reduce surface charging exist but are not well developed and are not in common usage. One suggestion for metallic surfaces is an oxide coating with a high secondary electron yield. This concept, in a NASCAP computer program simulation, reduced the absolute

charging of a spacecraft dramatically and reduced differential charging of shaded Kapton slightly. Any selected materials should be carefully analyzed to insure that they do not create problems of their own and that they work as intended over their service lives.

Another concept to reduce charging, the neutral plasma beam, is discussed in section 5.0.

3.1.3 Shielding

The primary spacecraft structure, electronic component enclosures, and electrical cable shields shall provide a physically and electrically continuous shielded surface around all electronics and wiring (Faraday cage). The primary spacecraft structure should be designed as an electromagnetic-interference-tight shielding enclosure (Faraday cage). The purposes of the shielding are (1) to prevent entry of space plasma into the spacecraft interior and (2) to shield the interior electronics from the radiated noise of an electrical discharge on the exterior of the spacecraft. All shielding should provide at least 40-dB attenuation of radiated electromagnetic fields associated with surface discharges. An approximately 1-mm thickness of aluminum or magnesium will generally provide the desired attenuation. This enclosure should be as free from holes and penetrations as possible. Many penetrations can be made relatively electromagnetic interference tight by use of well-grounded metallic meshes and plates. All openings, apertures, and slits shall be eliminated to maintain the integrity of the Faraday cage.

The metalization on multilayer insulation is insufficient to provide adequate shielding. Layers of aluminum foil mounted to the interior surface and properly grounded can be used to increase the shielding effectiveness of blankets or films. Aluminum honeycomb structures and aluminum facesheets can also provide significant attenuation. Electronic enclosures and electrical cables exterior to the main Faraday cage region should also be shielded to extend the coverage of the shielded region to 100 percent of the electronics.

Cable shields exterior to the Faraday cage shall maintain and extend the cage region from their exit/extrance of the main body of the spacecraft. Cable shields should be fabricated from aluminum or copper foil, sheet, or tape. Standard coaxial shielding or metalized plastic tape wraps on wires do not provide adequate shielding protection and should not be used. Shields shall be terminated when they enter the spacecraft structure from the outside and carefully grounded at the entry point. Braid shields on wires should be soldered to any overall shield wrap and grounded at the entrances to the spacecraft. Conventional shield grounding through a connector pin to a spacecraft interior location should not be used.

Electrical terminators, connectors, feedthroughs, and externally mounted components (diodes, etc.) should be electrically shielded and all shield caps tied to the common structural ground system of the space vehicle.

3.1.4 Filtering

Electrical filtering should be used to protect circuits from discharge-induced upsets. All circuits routed into the Faraday cage region, even though their wiring is in shielded cabling, run a higher risk of having ESD-caused transient voltages on them. Initial design planning should include ESD protection for these circuits. It is recommended that filtering be applied to these circuits unless analysis shows that it is not needed.

The usual criterion suggested for filtering is to eliminate noise below a specific time duration (i.e., above a specific frequency). On the Communications Technology Satellite (CTS), in-line transmitters and receivers were used that effectively eliminated noise pulses of less than 5-μs duration. Similar filtering concepts might include a voltage threshold or energy threshold. Filtering is believed to be an effective means of preventing circuit disruption and should be included in system designs. Any chosen filtering method should have analyses and tests to validate the selected criteria. Filters should be rated to withstand the peak transient voltages over the mission life.

3.1.5 Procedures

Proper handling, assembly, inspection, and test procedures shall be instituted to insure the electrical continuity of the space vehicle grounding system. The continuity of the space vehicle electrical grounding system is of great importance to the overall design susceptibility to spacecraft charging effects. In addition it will strongly affect the integrity of the space vehicle electromagnetic capability (EMC) design. Proper handling and assembly procedures must be followed during fabrication of the electrical grounding system. All ground ties should be carefully inspected and dc resistance levels should be tested during fabrication and again before delivery of the space vehicle. A final check of the ground system continuity during preparation for space vehicle launch is desirable.

3.2 Subsystem Guidelines

The guidelines in this section are divided by spacecraft subsystem. Designers of specific subsystems should read the applicable portions of this section and, in addition, review the general guidelines (table IV).

3.2.1 Electronics

The general guidelines apply.

3.2.2 Power systems

See table IV. In addition, the following specific guidelines apply.

3.2.2.1 Solar panel grounding.—**Solar array panels and substrates shall be electrically grounded to the structure.** Solar array panels and conductive sections of substrates and honeycomb should be grounded to each other with grounding jumpers and the entire network grounded to the space vehicle structure with less than 2.5-mΩ dc resistance per joint. Deployable panels on three-axis-stabilized vehicles can be grounded to the structure through sliprings where necessary. A ground wire can be used to bond together each lateral strip or row of solar cells.

3.2.2.2 Solar panel fabrication.—**Solar array panels shall use materials and fabrication techniques to minimize electrostatic discharge effects.** Solar panel back surfaces, edges, and honeycomb should be grounded conductors. Conductive black paint is suitable for the rear surface of the solar panel. Solar panel edges can be wrapped with grounded conductive tape. The front surface of the solar array consists of nonconductive coverslides and gaps sometimes potted with nonconductive adhesive for electrical design reasons. The potting thickness should be the minimum required. The front surfaces of coverslides may be coated with a conductive, transparent coating of grounded indium tin oxide if required. Such coatings typically reduce transmission by 5 to 10 percent and are generally used when absolute charging must be controlled.

3.2.2.3 Power system electrical design.—**Power system electrical design shall incorporate features to protect against transients due to electrical discharge.** Spark discharges from solar arrays should be anticipated, and the electrical design of the power system must provide adequate protection. The following design practices will help in reducing the effects of such spark discharges.

(1) Clamp solar array wiring, preferably at the entry to the spacecraft Faraday cage, but definitely before it enters the power supply.

(2) If solar array wiring is not clamped at the entry point to the Faraday cage, shield the wiring from that point to the power supply.

(3) Use solar array diodes with forward current ratings that anticipate expected ESD transient currents.

(4) Perform analysis and testing to verify the power system electrical design for survivability or immunity to spacecraft charging effects.

3.2.3 Mechanical and structural

See table IV. In addition, the following specific guideline applies: **Conductive honeycomb and facesheets shall be electrically grounded to the structure.**

Aluminum honeycomb substructures require special consideration for electrical grounding. Techniques for grounding conductive honeycomb and facesheets include rivets, copper wires, and metal inserts.

Care should be taken to establish ground ties at several locations on the honeycomb structure and to maintain ground continuity through all honeycomb parts and facesheets. For example, a recommended method of using copper wires involves sewing the wires transversely at shallow inclination angles through the honeycomb (making contact with several of the cell walls). The wires should be installed at maximum intervals of 30 cm across the structure. Ground wires should then be bolted to the structure. Electrical inspection of grounding interfaces for honeycomb structures applies.

3.2.4 Thermal control

See table IV. In addition, the following specific guidelines apply:

3.2.4.1 Thermal blankets.—**All metalized surfaces in multilayer insulation (MLI) blankets shall be electrically**

TABLE IV. - SUBSYSTEM GUIDELINES - APPLICABLE SECTIONS

Subsystem and design technology	Applicable sections					
	3.1.1	3.1.2	3.1.3	3.1.4	3.1.5	Extra
Electronics	X	X	X	X	X	
Power	X	X	X	X	X	3.2.2
Mechanical and structure	X		X		X	3.2.3
Thermal	X	X			X	3.2.4
Radiofrequency and communications	X	X	X	X	X	3.2.5
Attitude control	X	X	X	X	X	3.2.6
Payloads	X	X	X	X	X	3.2.7

grounded to the structure. The metalized multilayer surfaces should be electrically grounded to each other by ground tabs at the blanket edges. Each tab should be made from a 2.5-cm-wide strip of 0.005-cm-thick aluminum foil. The strip should be accordion folded and interleaved between the blanket layers to give a 2.5- by 2.5-cm contact area with all metalized surfaces and the blanket front and back surfaces. Nonconductive spacer or mesh material must be removed from the vicinity of the interleaved tab. The assembly should be held in place with a metallic nut and bolt that penetrates all blanket layers and captures 2.0-cm-diameter metallic washers positioned on the blanket front and back surfaces and centered in the 2.5- by 2.5-cm tab area. The washers may have different diameters, with the inner surface of the smaller washer recessed to insure maximum peripheral contact area between the interleaved foil strip and each metalized blanket surface. The tab should be grounded to structure by a proven technique such as a wire that is as short as possible (15 cm maximum) or conductive Velcro.

Redundant grounding tabs on all blankets are required as a minimum. Tabs should be located on blanket edges and spaced to minimize the maximum distance from any point on the blanket to the nearest tab. Extra tabs may be needed on odd-shaped blankets to meet one additional condition: any point on a blanket should be within 1 m of a ground tab.

The following practices should be observed during blanket design, fabrication, handling, installation, and inspection:

(1) Verify layer-to-layer blanket grounding during fabrication.

(2) After installation, verify less than 10-Ω dc resistance between blanket and structure.

(3) Close blanket edges (cover, fold in, or tape) to prevent direct irradiation of inner layers.

(4) Do not use crinkled, wrinkled, or creased metalized film material.

(5) Handle blankets carefully to avoid creasing of the film or possible degradation of the ground tabs.

(6) If the blanket exterior is conductive (paint, indium tin oxide, "fog"), make sure that it contacts the ground tab.

3.2.4.2 Thermal control louvers.—**Ground the blades of thermal control louvers.** A fine wire with minimal torque behavior or a fine slip brush can do the job with acceptable torque constraints.

3.2.5 Communications systems

See table IV. In addition, the following specific guidelines apply.

3.2.5.1 Antenna grounding.—**Antenna elements shall be electrically grounded to the structure.** Implementation of antenna grounding will require careful consideration in the initial design phase. All metal surfaces, booms, covers, and feeds should be grounded to the structure by wires and metallic screws (dc short design). All waveguide elements should be electrically bonded together with spotwelded connectors and grounded to the spacecraft structure. These elements must be grounded to the Faraday cage at their entry points. Conductive epoxy can be used where necessary, but dc resistance of about 1 Ω must be verified by measurements.

3.2.5.2 Antenna apertures.—**Spacecraft rf antenna aperture covers shall be ESD conductive and grounded.** Charging and arcing of dielectric antenna dish surfaces and radomes can be prevented by covering them with grounded ESD-conductive material. Antenna performance should be verified with the ESD covering installed.

3.2.5.3 Antenna reflector surfaces.— **Grounded, conductive spacecraft charge control materials shall be used on antenna reflector rear surfaces.** Appropriate surface covering techniques must be selected. Applicable methods include conductive meshes bonded to dielectric materials, silica cloth, conductive paints, or nonconductive (but charge bleeding) paints overlapping grounded conductors.

3.2.5.4 Transmitters and receivers.—**Spacecraft transmitters and receivers (command line and data line) shall be immune to transients produced by electrostatic discharge.** Transmitter and receiver electrical design must be compatible with the results of spacecraft charging effects. The EMI environment produced by spacecraft electrostatic discharge should be addressed early in the design phase to permit effective electrical design for immunity to this environment. The transmitter, receiver, and antenna system should be tested for immunity to ESD's near the antenna feed. The repetition rate shall be selected to be consistent with estimated arc rates of nearby materials.

3.2.6 Attitude control

Attitude control electronics packages should be insensitive to ESD transients. See table IV. Attitude control systems often require sensors that are remote from electronics packages for Faraday shielding. This presents the risk that ESD transients will be picked up and conducted into electronics. Particular care must be taken to insure immunity to ESD upset in such cases.

3.2.7 Payloads

See table IV. In addition, the following specific guidelines apply.

3.2.7.1 Deployed packages.—**Deployed packages shall be grounded by using a flat ground strap extending the length of the boom to the vehicle structure.** Several spacecraft designs incorporate dielectric booms to deploy

payloads. The payload electrical system may still require a common ground reference, or the experiment may require a link to some electric potential reference. In these cases it is recommended that a flat ground strap be used to carry this ground tie to the vehicle structure. Electrical wiring extending from the deployed payload to the spacecraft interior must be carried inside or along the dielectric booms. This wiring should be shielded and the shield grounded at the package end and at the Faraday cage entrance.

3.2.7.2 Ungrounded materials.—**Specific items that cannot be grounded because of system requirements shall undergo analysis to assure specified performance in the spacecraft charging environment.** Certain space vehicles may contain specific items or materials that must not be grounded. For example, a particular experiment may have a metallic grid or conducting plate that must be left ungrounded. If small, these items may present no unusual spacecraft charging problems; however, this should be verified through analysis.

3.2.7.3 Deliberate surface potentials.—**If a surface on the spacecraft must be charged (detectors on a science instrument, for example), it shall be recessed or shielded so that the perturbance in surface electrostatic potentials is less than 10 V.** Scientific instruments with the need for exposed surface voltages for measurement purposes, such as Faraday cups, require special attention to insure that the electrostatic fields they create will not disrupt adjacent surface charging or cause discharges by their operation. They can be recessed so their fields at the spacecraft surface are minimal or shielded with grounded grids. An analysis may be necessary to insure that their presence is tolerable from a spacecraft charging standpoint.

4.0 Spacecraft Test Techniques

Spacecraft and systems should be subjected to transient upset tests to verify immunity. It is the philosophy in this document that testing is an essential ingredient in a sound spacecraft charging protection program. In this section the philosophy and methods of testing spacecraft and spacecraft systems are reviewed.

4.1 Test Philosophy

The philosophy of the ESD test is identical to that of the normal environmental qualification test:

(1) Subject the spacecraft to an environment representative of that expected.

(2) Make the environment applied to the spacecraft more severe than expected as a safety margin to give confidence that the flight spacecraft will survive the real environment.

(3) Have a design qualification test sequence that is extensive: test all units of hardware, use long test durations, examine many equipment operating modes, apply the environment to all surfaces of the test unit.

(4) Have a flight hardware test sequence of more modest scope: delete some units from test if qualification tests show great design margins, use shorter test durations, use only key equipment operating modes, and apply the environment to a limited number of surfaces.

Ideally, both prototype and flight spacecraft should be tested in a charging simulation facility. They should be electrically isolated from ground and bombarded with electron, ion, and extreme ultraviolet radiation levels corresponding to substorm environment conditions. Systems should operate without upset throughout this test.

Because of the difficulty of simulating the actual environment (space vacuum and plasma parameters including species such as ions, electrons, and heavier ions; mean energy; energy spectrum; and direction), spacecraft charging tests usually take the form of assessing unit immunity to electrical discharge transients. The appropriate discharge sources are based on separate estimates of discharge parameters.

Tests in a room ambient environment employing radiated and injected transients are more convenient. However, these ground tests cannot simulate all effects of the real environment because the transient source may not be in the same location as the region that may discharge and because a spark in air has a slower risetime than a vacuum arc. The sparking device's location and pulse shape must be analyzed to provide the best possible simulation of coupling to electronic circuits. To account for the difference in risetime, the peak voltage might be increased to simulate the dV/dt parameter of a vacuum arc. Alternatively the voltage induced during a test could be measured and the in-flight noise extrapolated from the measured data.

A proper risk assessment will involve a well-planned test, predictions of voltage stress levels at key spacecraft components, verification of these predictions during test, checkout of the spacecraft after test, and collaboration with all project elements to coordinate and assess the risk factors.

4.2 Simulation of Parameters

Because ESD test techniques are not well established, it is important to understand the various parameters that must be simulated, at a minimum, to perform an adequate test. On the basis of their possibility of interference to the spacecraft, the following items should be considered in designing tests:

(1) Spark location
(2) Radiated fields or structure currents

(3) Area, thickness, and dielectric strength of the material

(4) Total charge involved in the event

(5) Breakdown voltage

(6) Current waveform: risetime, width, falltime, and rate of rise (in amperes per second)

(7) Voltage waveform: risetime, width, falltime, and rate of rise (in amperes per second)

Table V shows typical values as calculated on some spacecraft. The values listed in this table were compiled from a variety of sources, mostly associated with the Voyager and Galileo spacecraft. The values for each item (e.g., those for the dielectric plate) have been assembled from the best available information and made into a more or less self-consistent set of numbers. The process is described in the footnotes to table V. See the bibliography for further description and discussion.

4.3 General Test Methods

4.3.1 ESD-generating equipment

Several representative types of test equipment are described in table VI. Where possible, typical parameters for that type of test are listed.

4.3.1.1 MIL-STD-1541 arc source.—The Military Standard 1541 (MIL-STD-1541) arc source is commonly used. The schematic and usage instructions extracted from MIL-STD-1541 are presented here as figure 11. The arc source can be manufactured relatively easily and can provide some of the parameters necessary to simulate a space-caused ESD event. The only adjustable parameter for the MIL-STD-1541 arc source is the discharge voltage (achieved by adjusting the discharge gap and, if necessary, the dc supply to the discharge capacitor). As a result, peak current and energy vary with the discharge voltages. Since the risetime, pulse width, and falltime are more or less constant, the voltage and current rates of rise and fall are not independent parameters. This permits some degree of flexibility in planning tests but not enough to cover all circumstances.

4.3.1.2 Flat-plate capacitor.—A flat-plate capacitor can be used in several circumstances. Examples of spacecraft areas that can be simulated by a flat-plate capacitor are (1) thermal blanket areas, (2) dielectric areas such as calibration targets, and (3) dielectric areas such as nonconductive paints. The chief value of a flat-plate capacitor is to permit a widespread discharge to simulate the physical path of current flow. This can be of significance where cabling or circuitry is near the area in question. Also, the larger size of the capacitor plates allows them to act as an antenna during discharge and thus produce significant radiated fields.

Table VI shows one example of the use of a flat-plate capacitor. Several parameters can be varied, chiefly the area and the dielectric thickness; both of these affect the capacitance, the discharge current, and the energy. The

TABLE V. – EXAMPLES OF ESTIMATED SPACE-GENERATED ESD SPARK PARAMETERS

ESD generator	Capacitance,[a] C, nF	Breakdown voltage,[b] V_B, kV	Energy,[c] E, mJ	Peak current,[d] I_{pk}, A	Discharge current risetime,[e] t_r, ns	Discharge current pulse width,[f] t_p, ns
Dielectric plate to conductive substrate	20	1	10	2[g]	3	10
Exposed connector dielectric	.150	5	1.9	36	10	15
Paint on high-gain antenna	550	1	150	150	5	2400
Conversion coating on metal plate	4.5	1	2.25	16	20	285
Paint on optics hood	550	.360	35 000	18	5	600

[a]Computed from surface area, dielectric thickness, and dielectric constant.
[b]Computed from dielectric thickness and material breakdown strength.
[c]Computed from $E = 1/2\ CV^2$
[d]Estimated based on measured data; extrapolation based on square root of area.
[e]Measured and deduced from test data.
[f]To balance total charge on capacitor.
[g]This was replacement current in longer ground wire; charge is not balanced.

TABLE VI. - EXAMPLES OF SEVERAL ESD GENERATORS

ESD generator	Capacitance,[a] C, nF	Breakdown voltage, V_B, kV	Energy, E, mJ	Peak current, I_{pk}, A	Discharge current risetime, t_r, ns	Discharge current pulse width, t_p, ns
MIL-STD-1541 (auto coil)[a]	0.035	19	6	80	5	20
Flat plate 20 cm x 20 cm at 5 kV, 0.08 mm (3 mil) Mylar insulation	14	5	180	80	35	880
Flat plate with lumped-element capacitor	550	.450	55	15	15	(b)
Capacitor direct injection	1.1	320	.056	1	3×10^9 to 10×10^9	20
Capacitor arc discharge	60	1.4	59	1000	(c)	80

[a]Parameters were measured on one unit similar to the MIL-STD-1541 design.
[b]RC time constant decay.
[c]Value uncertain.

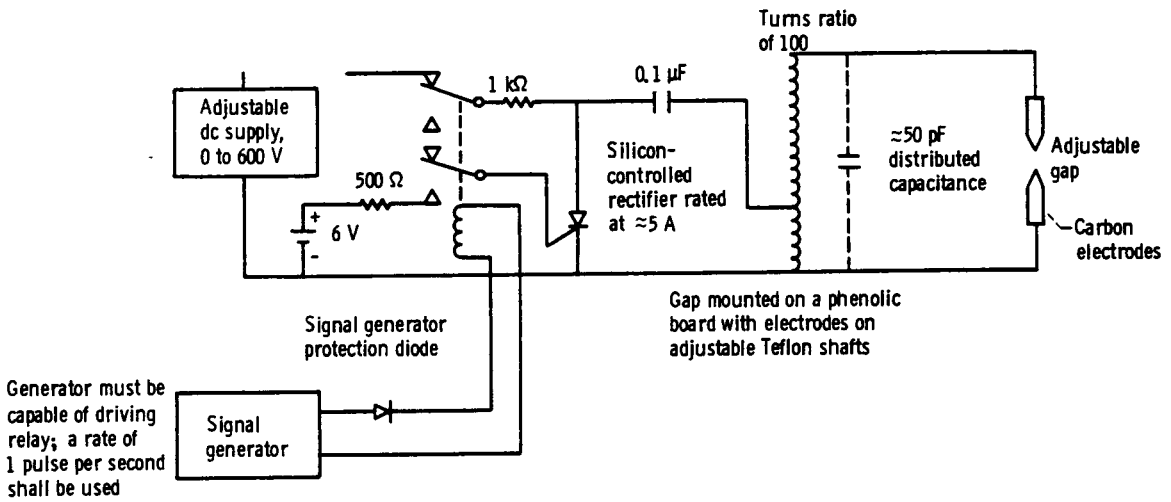

Typical gap-spacing and voltage breakdown level

Gap, mm	Voltage breakdown, kV	Approximate energy dissipated, W
1	1.5	56.5×10^{-6}
2.5	3.5	305
5	6	900
7.5	9	2000

Figure 11.—Schematic diagram of MIL-STD-1541 arc source.

discharge voltage of the flate plate can be controlled by using a needlepoint discharge gap at its edge that is calibrated to break down before the dielectric. This gap also affects discharge energy. In this manner, several mechanical parameters can be designed to yield discharge parameters more closely tailored to those expected in space.

The difficulties of this method include the following:

(1) The test capacitor is usually not as close to the interior cabling as the area it is intended to simulate (e.g., it cannot be placed as close as the paint thickness).

(2) The capacitance of the test capacitor may be less than that of the area it is intended to simulate. To avoid uncontrolled dielectric breakdown in the test capacitor, its dielectric may have to be thicker than the region it simulates. If so, the capacitance will be reduced. The area of the test capacitor can be increased to compensate, but then the size and shape will be less realistic.

4.3.1.3 Lumped-element capacitors.—Use of lumped-element capacitors can overcome some of the objections raised about flat-plate capacitors. They can have large capacitances in smaller areas and thus supplement a flat-plate capacitor if it alone is not adequate. The deficiencies of lumped-element capacitors are as follows:

(1) They generally do not have the higher breakdown voltages (greater than 5 kV) needed for ESD tests.

(2) Some capacitors have a high internal resistance and cannot provide the fast risetimes and peak currents needed to simulate ESD events.

Generally, the lumped capacitor discharge would be used most often in lower voltage applications (to simulate painted or anodized surface breakdown voltages) and in conjunction with the flat-plate capacitors.

4.3.1.4 Other source equipment.—Wilkenfeld et al. (1982) describes several other similar types of ESD simulators. It is a useful document if further descriptions of ESD testing are desired.

4.3.1.5 Switches.—A wide variety of switches can be used to initiate the arc discharge. At low voltages, semiconductor switches can be used. The MIL-STD-1541 arc source uses an SCR to initiate the spark activity on the primary of a step-up transformer; the high voltage occurs at an air spark gap on the transformer's secondary. Also at low voltages, mechanical switches can be used (e.g., to discharge modest-voltage capacitors). The problem with mechanical switches is their "bounce" in the early milliseconds. Mercury-wetted switches can alleviate this problem to a degree.

For high-voltage switching in air, a gap made of two pointed electrodes can be used as the discharge switch. Place the tips pointing toward each other and adjust the distance between them to about 1 mm/kV of discharge voltage. The gap must be tested and adjusted before the test, and it must be verified that breakdown occurred at the desired voltage. For tests that involve a variable amplitude, a safety gap connected in parallel is suggested. The second gap should be securely set at the maximum permissible test voltage. The primary gap can be adjusted during the test from zero to the maximum voltage desired without fear of inadvertent overtesting. The test is performed by charging the capacitor (or triggering the spark coil) and relying on the spark gap to discharge at the proper voltage.

The arc source's power supply must be sufficiently isolated from the discharge so that the discharge is a transient and not a continuing arc discharge. A convenient test rate is once per second. To accomplish this rate, it is convenient to choose the capacitor and isolation resistor's resistance-capacitance time constant to be about 1/2 second and to make the high-voltage power supply output somewhat higher than the desired discharge voltage.

For tests that involve a fixed discharge voltage, gas discharge tubes are available with fixed breakdown voltages. The advantage of the gas discharge tube over needlepoints in air is its faster risetime and its very repeatable discharge voltage. The gas discharge tube's dimensions (5 to 7 cm or longer) can cause more radio-frequency radiation than a smaller set of needlepoint air gaps.

Another type of gas discharge tube is the triggered gas discharge tube. This tube can be triggered electronically, much as an SCR can be turned on by its gate. This method has the added complexity of the trigger circuitry. Additionally, the trigger circuitry must be properly isolated so that discharge currents are not diverted by the trigger circuits.

4.3.2 Methods of ESD application

The ESD energy can range from very small to large (as much as 1 J but usually millijoules). The methods of application can range from indirect (radiated) to direct (applying the spark directly to a piece part). In general, the method of application should simulate the expected ESD source as much as possible. Several typical methods are described here.

4.3.2.1 Radiated field tests.—The sparking device can be operated in air at some distance from the component. This technique can be used to check for rf interference to communications or surveillance receivers as coupled into their antennas. It can also be used to check the susceptibility of scientific instruments that may be measuring plasma or natural radio waves. Typical rf-radiated spectra are shown in figure 12.

4.3.2.2 Single-point discharge tests.—Discharging an arc onto a spacecraft surface (or a temporary protective metallic fitting), with the arc current return wire in close proximity, can represent the discharge and local flowing of arc currents. This test is more severe than the radiated

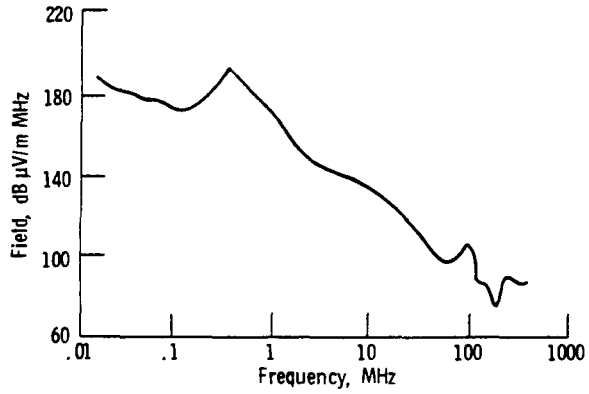

Figure 12.—Typical radiofrequency-radiated fields from MIL-STD-1541 arc source.

test, since it is performed immediately adjacent to the spacecraft rather than some distance away.

This test simulates only local discharge currents; it does not simulate "blowoff" of charges, which causes currents in the entire structure of the spacecraft.

4.3.2.3 Structure current tests.—The objective of structure current testing is to simulate "blowoff" of charges from a spacecraft surface. If a surface charges, and a resultant ESD occurs, the spark may vaporize and mechanically remove material and charges without local charge equalization. In such a case the remaining charge on the spacecraft will redistribute itself and cause structural currents.

Defining the actual blowoff currents and the paths they take is difficult. Nevertheless, it is appropriate to do a structure current test, to determine the spacecraft susceptibility, by using test currents and test locations supported by analysis as illustrated in sections 2.2 and 2.3. Typically, such a test would be accomplished by using one or more of the following current paths (fig. 13):

(1) Diametrically opposed locations (through the spacecraft)

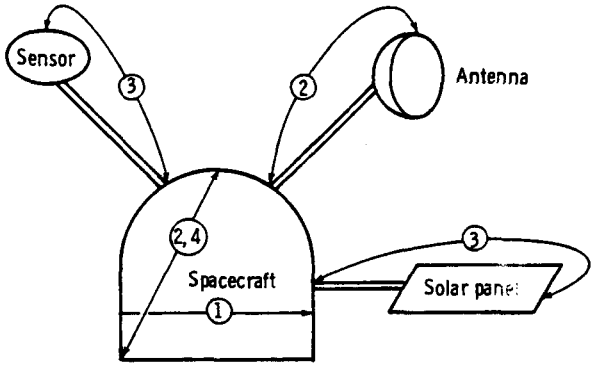

Figure 13.—Paths for electrostatic discharge currents through structure.

(2) Protuberances (from landing foot to top from antenna to body, and from thruster jets to opposite side of body)

(3) Extensions or booms (from end of sensor boom to spacecraft chassis and from end of solar panel to spacecraft chassis)

(4) From launch attachment point to other side of spacecraft

The test using current path 1 is of general nature. Tests using current paths 2 and 3 simulate probable arc locations on at least one end of the current path. These test points include thrusters, whose operation can trigger an incipient discharge, and landing feet and the attachment points, especially if used in a docking maneuver, when they could initiate a spark to the mating spacecraft.

Test 3 is an especially useful test. Solar panels often have glass (nonconductive) coverslides, and sensors may have optics (nonconductive) that can cause an arc discharge. In both cases, any blowoff charge would be replaced by a current in the supporting boom structure that could couple into cabling in the boom. This phenomenon is possibly the worst-case event that could occur on the spacecraft because the common length of the signal or power cable near the arc current is the longest on the spacecraft.

4.4 Unit Testing

4.4.1 General

Unit ESD testing serves the same purpose it serves in standard environmental testing (i.e., it identifies design deficiencies at a stage when the design is more easily changed). However, it is very difficult to provide a realistic determination of the unit's environment as caused by an ESD on the spacecraft.

A unit testing program could specify a single ESD test for all units or could provide several general categories of test requirements. The following test categories are provided as a guide:

(1) Internal units (general) must survive, without damage or disruption, the MIL-STD-1541 arc source test (discharges to the unit but no arc currents through the unit's chassis).

(2) External units mounted outside the Faraday cage (usually exterior sensors) must survive the MIL-STD-1541 arc source at a 5-kV level with discharge currents passing from one corner to the diagonally opposite corner (four pairs of locations).

(3) For units near a known ESD source (solar cell coverslides, Kapton thermal blankets, etc.), the spark voltage and other parameters must be tailored to be similar to the expected spark from that dielectric surface.

4.4.2 Unit test configuration

ESD tests of the unit ("subsystem") can be performed with the subsystem configured as it would be for a standard electromagnetic compatibility (EMC) radiated susceptibility test. The unit is placed on and electrically bonded to a grounded copper-topped bench. The unit is cabled to its support equipment, which is in an adjacent room. The unit and cabling should be of flight construction with all shields, access ports, etc., in flight condition. All spare cables should be removed.

4.4.3 Unit test operating modes

The unit should be operated in all modes appropriate to the ESD arcing situation. Additionally, the unit should be placed in its most sensitive operating condition (amplifiers in highest gain state, receivers with a very weak input signal) so that the likelihood of observing interference from the spark is maximized. The unit should also be exercised through its operating modes to assure that mode change commands are possible in the presence of arcing.

4.5 Spacecraft Testing

The system level test will provide the most reliable determination of the expected performance of a space vehicle in the charging environment. Such a test should be conducted on a representative spacecraft before exposing the flight spacecraft to insure that there will be no inadvertent overstressing of flight units.

A detailed test plan must be developed that defines test procedures, instrumentation, test levels, and parameters to be investigated. Test techniques will probably involve current flow in the spacecraft structure. Tests can be conducted in ambient environments, but screen rooms with electromagnetic dampers are recommended. MIL-STD-1541 system test requirements and radiated electromagnetic interference testing are considered to be a minimal sequence of tests.

The spacecraft should be isolated from ground. Instrumentation must be electrically screened from the discharge test environment and must be carefully chosen so that instrument response is not confused with spacecraft response. The spacecraft and instrumentation should be on battery power. Complete spacecraft telemetry should be monitored. Voltage probes, current probes, E and H shield current monitors, and other sensors should be installed at critical locations. Sensor data should be transmitted with fiber optic data links for best results. Oscilloscopes and other monitoring instruments should be capable of resolving the expected fast response to the discharges ($\leq$250 MHz).

The test levels should be determined from analysis of discharging behavior in the substorm environment. It is recommended that full level testing, with test margins, be applied to structural, engineering, or qualification models of spacecraft with only reduced levels applied to flight units. The test measurements (structural currents, harness transients, upsets, etc.) are the key system responses that are to be used to validate predicted behavior.

4.5.1 General

Spacecraft testing is generally performed in the same fashion as unit testing; a test plan of the following sort is typical:

(1) The MIL-STD-1541 radiated test is applied around the entire spacecraft.

(2) Spark currents from the MIL-STD-1541 arc source are applied through spacecraft structure from launch vehicle attachment points to diagonally opposite corners.

(3) ESD currents are passed down the length of booms with cabling routed along them (e.g., sensor booms or power booms). Noise pickup into cabling and circuit disruption are monitored.

(4) Special tests are devised for special situations. For example, dielectric regions such as quartz second-surface mirrors, Kapton thermal blankets, and optical viewing windows should have ESD tests applied on the basis of their predicted ESD characteristics.

4.5.2 Spacecraft test configuration

The spacecraft ESD testing configuration ideally simulates a 100 percent flight-like condition. This may be difficult because of the following considerations:

(1) Desire for ESD diagnostics in the spacecraft

(2) Nonfunctioning power system

(3) Local rules about grounding the spacecraft to facility ground

(4) Cost and schedules to completely assemble the spacecraft for the test and later disassemble it

(5) The possible large capacitance to ground of the spacecraft in its test fixture

(6) ESD coupling onto nonflight test cabling

4.5.2.1 Test diagnostics.—To obtain more information about circuit response than can be obtained by telemetry, it is common to measure induced voltages due to the ESD test sparks at key circuits. If improperly implemented, the very wires that access the circuits and exit the spacecraft to test equipment (e.g., oscilloscopes) will act as antennas and show noise that never would be present without those wires.

Two approaches have been used with some success. The first is using conventional oscilloscope probes, with great care. Long oscilloscope probes (3 m) were procured from Tektronix. For the circuits being monitored, a small "tee" breakout connector was fabricated and inserted at the connecter nearest the circuit. Two oscilloscope probes were attached to each circuit's active and return wires and the probe tips were grounded to satellite structure in the immediate vicinity of the breakout tee. The probe grounds were less than 15 cm from the probe tip. The signal was measured on a differential input of the oscilloscope. Before installation the probes were capacitively compensated to their respective oscilloscope preamplifiers, and it was verified that their common-mode voltage rejection was adequate (in short, normal good practice). The two probe leads were twisted together and routed along metal structure inside the satellite until they could be routed out of the main chassis enclosure. They were then routed (still under thermal blankets) along structure to a location as remote as possible from any ESD test location and finally were routed to the oscilloscope. The oscilloscopes were isolated from building ground by isolation transformers. Clearly, this method permits monitoring only a few circuits.

A second method of monitoring ESD-induced voltage waveforms on internal circuits is the use of battery-powered devices that convert voltages to light-emitting diode (LED) signals. The LED signals can be transmitted by fiber optics to exterior receiving devices, where the voltage waveform is reconstructed. As with the oscilloscope probes, the monitoring device must be carefully attached to the wires with minimal disturbance to circuit wiring. The fiber optics cable must be routed out of the satellite with minimal disturbance. The deficiency of such a monitoring scheme is that the sending device must be battery powered, turned on, and installed in the spacecraft before spacecraft buildup and must operate for the duration of the test. The need for batteries and the high power consumption of LED's severely restrict this method.

Another proposed way to obtain circuit response information is to place peak-hold circuitry at key circuits, installed as described above. This method is not very useful because the only datum presented is that a certain peak voltage occurred. There is no evidence that the ESD test caused it, and there is no way to correlate that voltage with any one of the test sequences. For analysis purposes, such information is worthless.

4.5.2.2 Nonfunctioning power system.—Spacecraft using solar cells or nuclear power supplies often must use support equipment power supplies for ground test activities and thus are not totally isolated from ground. In such cases the best work-around is to use an isolated and balanced output power supply with its wires routed to the spacecraft at a height above ground to avoid stray capacitance to ground. The power wires should be shielded to avoid picking up stray radiated ESD noise; the shields should be grounded at the support equipment end of the cable only.

4.5.2.3 Facility grounding.—To simulate flight, the spacecraft should be isolated from ground. Normal test practice dictates an excellent connection to facility ground. For the purposes of this test a temporary ground of 0.2 to 2 MΩ or more will isolate the spacecraft for the purposes of the ESD test. Generally 0.2 to 2 MΩ is sufficient "grounding" for special test circumstances of limited duration and can be tolerated for the ESD test.

4.5.2.4 Cost and schedules to assemble and disassemble spacecraft.—Often testing is done in the most compact form possible, attempting to interleave several tasks at one time or to perform tasks in parallel. This practice is incompatible with the needs of ESD testing and must be avoided. A thermal vacuum test, for example, is configured like the ESD test, but has numerous (nonflight) thermocouple leads penetrating from the interior to the exterior of the spacecraft. These leads can act as antennas and bring ESD-caused noise into satellite circuitry, where it never would have been.

4.5.2.5 Spacecraft capacitance to ground during test.—If stray capacitance to facility ground is present during the ESD test, it will modify the flow of ESD currents. For an better test the spacecraft should be physically isolated from facility ground. It can be shown that raising a 1.5-m-diameter spherical satellite 0.5 m off the test flooring reduces the stray capacitance nearly to that of an isolated satellite in free space. A dielectric (e.g., wood) support structure can be fabricated for the ESD test and will provide the necessary capacitive isolation.

4.5.2.6 ESD coupling onto nonflight test cabling.—One method of reducing ESD coupling to and

from the spacecraft on nonflight test wiring is the use of ferrite beads on all such wiring.

5.0 Control and Monitoring Techniques

5.1 Active Spacecraft Charge Control

Charge control devices are a means of controlling spacecraft potential. Various active charged-particle emitters have been and are being developed and show promise of controlling spacecraft potential in the space plasma environment. At this time only neutral plasma devices (both ion and electron emitters) have demonstrated the ability to control spacecraft potential in geomagnetic substorms. These devices are recommended for charge control purposes (Purvis and Bartlett, 1980; Olsen, 1978; Olsen and Whipple, 1977).

Emitted particles constitute an additional term in the current balance of a spacecraft. Because the ambient current densities at geosynchronous altitude are quite small, emitting small currents from a spacecraft can have a strong effect on its potential, as has been demonstrated on the Applications Technology Satellites ATS-5 and ATS-6, Spacecraft Charging at High Altitudes (SCATHA), and other spacecraft. However, devices that emit particles of only one electric charge (e.g., electrons) are not suitable for active potential control applications unless all spacecraft surfaces are conducting. Activation of such a device will result in a rapid change of spacecraft potential. However, differential charging of any insulating surfaces will occur and cause potential barrier formation near the emitter. Emission of low-energy particles can then be suppressed. Higher energy particles can escape, but their emission could result in the buildup of large differential potentials. On the other hand, devices that emit neutral plasmas or neutralized beams (e.g., hollow cathode plasma sources or ion engines) can maintain spacecraft potentials near plasma ground and suppress differential charging. These are therefore the recommended types of charge control devices.

5.2 Environmental and Event Monitors

The occurrence of environmentally induced discharge effects in spacecraft systems is usually difficult to verify. An anomaly is known only to have occurred at some time. Since most spacecraft are not well instrumented for environmental effects, the state of the environment at the time of the anomaly would have to be inferred from ground observatory data. These environmental data are not necessarily the same at the spacecraft location; in fact, the correlation is generally poor.

This unknown condition could be modified if spacecraft carried a set of spacecraft charging effect monitors. A simple monitor set has been designed that will measure the characteristic energy and current flux of the environment as well as determine transients on four harness positions within the spacecraft (Sturman, 1981). This will allow correlation between the onset of the substorm environment and possible transients induced on the electronic systems. This package weighs about 1.4 kg and uses less than 3 W of power. The environment sensors would have to be on the outside surfaces and preferably in shade.

More sophisticated packages are available. Ion particle detectors in the range 10 to 50 keV could be used to sense the onset of geomagnetic substorms. Transient monitors capable of measuring the pulse characteristics are also available (Koons, 1981). These would require larger weight and power budgets but do provide better data.

These spacecraft charging effect monitors require data analysis support in order to produce the desired results. If they were carried on a number of operational satellites, the technology community would be able to obtain a statistical base relating charging to induced transients. The operational people, on the other hand, would be able to tell when charging is of concern, to establish procedures minimizing detrimental effects, and to separate system malfunctions from environmentally induced effects.

It is recommended that monitor packages be carried on all geosynchronous spacecraft. These packages must consist of both environment and transient pulse detectors.

National Aeronautics and Space Administration
Lewis Research Center
Cleveland, Ohio, April 16, 1984

Appendix A

Description of Geosynchronous Plasma Environments

In section 2.0 of this document geosynchronous plasma environments are briefly introduced and simply described in terms of temperature and number density. The environment is actually very complex and dynamic and not yet fully understood even by researchers. The simple characterization of the environment in section 2.0 uses only two species, electrons and protons; it assumes a "single Maxwellian" distribution, where the energy distribution of each species is considered to be described by the mathematical function, the "Maxwellian." The Maxwellian treatment is used because the function can be easily treated in the necessary mathematical manipulations for calculating spacecraft charging. If a Maxwellian is not used, measured data must be curve fit digitally and at much greater computational cost. If a single-Maxwellian distribution is inadequate for a given circumstance, the measured data are often treated as the sum of two populations, each with a Maxwellian distribution: the "two Maxwellian" characterization. Other species such as oxygen and helium can be treated as additional Maxwellian populations. The following text describes in greater detail different characterizations of the geosynchronous plasma environment.

Characterizations of Geosynchronous Plasma Environment

An initial step in looking at an environment is to consider averages. Ten-minute averages of approximately 45 days (per spacecraft) were made of data for the ATS-5, ATS-6, and SCATHA (experiment SC9) spacecraft (table VII); isotropy was assumed. The standard deviations present in the data were estimated (table VIII). The ions were assumed to be protons in these tables. Note that in many cases the standard deviation exceeded the average. This resulted from the great variability of the geosynchronous environment and illustrates the inherent difficulty of attempting to characterize the "average" plasma environment. These values are useful, however, in estimating the prestorm conditions that a spacecraft will experience. As the initial charge state of a spacecraft is important in determining how the vehicle will respond to a significant environmental perturbation, this is useful information. Also these averages give an approximate idea of how plasma conditions vary over a solar cycle since the ATS-5 data are for 1969-70, the ATS-6 data for 1974-76, and the SCATHA data for 1978.

TABLE VII. - AVERAGE PARAMETERS

(a) Electrons

Parameter	Spacecraft		
	ATS-5	ATS-6	SCATHA
Number density, $\langle ND \rangle$, cm^{-3}	0.80	1.06	1.09
Current density, $\langle J \rangle$, nA cm^{-2}	0.068	0.096	0.115
Energy density, $\langle ED \rangle$, eV cm^{-3}	1970	3590	3710
Energy flux, $\langle EF \rangle$, eV cm^{-2} s^{-1} sr^{-1}	0.98×10^{12}	2.17×10^{12}	1.99×10^{12}
Number density for population 1, N_1, cm^{-3}	0.578	0.751	0.780
Temperature for population 1, T_1, keV	0.277	0.460	0.550
Number density for population 2, N_2, cm^{-3}	0.215	0.273	0.310
Temperature for population 2, T_2, keV	7.04	9.67	8.68
Average temperature, T_{av}, keV	1.85	2.55	2.49
Root-mean-square temperature, T_{rms}, keV	3.85	6.25	4.83

(b) Ions

Number density, $\langle ND \rangle$, cm^{-3}	1.30	1.20	0.58
Current density, $\langle J \rangle$, pA cm^{-2}	5.1	3.4	3.3
Energy density, $\langle ED \rangle$, eV cm^{-3}	13 000	12 000	9440
Energy flux, $\langle EF \rangle$, eV cm^{-2} s^{-1} sr^{-1}	2.6×10^{11}	3.4×10^{11}	2.0×10^{11}
Number density for population 1, N_1, cm^{-3}	0.75	0.93	0.19
Temperature for population 1, T_1, keV	0.30	0.27	0.80
Number density for population 2, N_2, cm^{-3}	0.61	0.33	0.39
Temperature for population 2, T_2, keV	14.0	25.0	15.8
Average temperature, T_{av}, keV	6.8	12.0	11.2
Root-mean-square temperature, T_{rms}, keV	12.0	23.0	14.5

TABLE VIII. - STANDARD DEVIATIONS

(a) Electrons

Parameter	Spacecraft		
	ATS-5	ATS-6	SCATHA
Number density, ⟨ND⟩, cm^{-3}	± 0.79	± 1.1	± 0.89
Current density, ⟨J⟩, nA cm^{-2}	∓ 0.088	∓ 0.09	∓ 0.10
Energy density, ⟨ED⟩, eV cm^{-3}	± 3100	∓ 3700	∓ 3400
Energy flux, ⟨EF⟩, eV cm^{-2} s^{-1} sr^{-1}	$\pm 1.7 \times 10^{12}$	$\pm 2.6 \times 10^{12}$	$\pm 2.0 \times 10^{12}$
Number density for population 1, N_1, cm^{-3}	± 0.55	± 0.82	± 0.70
Temperature for population 1, T_1, keV	∓ 0.17	∓ 0.85	∓ 0.32
Number density for population 2, N_2, cm^{-3}	∓ 0.38	∓ 0.34	∓ 0.37
Temperature for population 2, T_2, keV	± 2.1	± 3.6	± 4.0
Average temperature, T_{av}, keV	± 2.0	± 2.0	± 1.5
Root-mean-square temperature T_{rms}, keV	∓ 3.3	∓ 3.5	∓ 2.9

(b) Ions

Number density, ⟨ND⟩, cm^{-3}	± 0.69	± 1.7	± 0.35
Current density, ⟨J⟩, pA cm^{-2}	± 2.7	∓ 1.8	± 2.1
Energy density, ⟨ED⟩, eV cm^{-3}	∓ 9700	∓ 9100	∓ 6820
Energy flux, ⟨EF⟩, eV cm^{-2} s^{-1} sr^{-1}	$\pm 3.5 \times 10^{11}$	$\pm 3.6 \times 10^{11}$	$\pm 1.7 \times 10^{11}$
Number density for population 1, N_1, cm^{-3}	± 0.54	± 1.78	± 0.16
Temperature for population 1, T_1, keV	∓ 0.30	∓ 0.88	± 1.0
Number density for population 2, N_2, cm^{-3}	∓ 0.33	∓ 0.16	∓ 0.26
Temperature for population 2, T_2, keV	± 5.0	± 8.5	± 5.0
Average temperature, T_{av}, keV	± 3.6	± 8.4	± 4.6
Root-mean-square temperature, T_{rms}, keV	∓ 4.8	∓ 8.9	∓ 5.3

A second way of considering environments is to look at "worst case" situations. Worst-case estimates of the parameters in table VII were made for the geosynchronous environment (table IX). These values were derived from fits to the plasma distributions observed during the several known worst-case charging events. The SCATHA spacecraft instrumentation allowed a breakout of the data into components parallel and perpendicular to the magnetic field and thus permited a more realistic representation of the actual environment. These values are particularly useful in estimating the extremes in environment that a geosynchronous spacecraft is likely to encounter.

A third quantity of interest in estimating the effects of the space environment on charging is the yearly percentage of occurrence of the plasma parameters. The occurrence frequencies of the temperature and current (fig. 14) were derived by fitting the observed distributions of electron and ion temperature for University of California at San Diego instruments on ATS-5, ATS-6, and SCATHA. The current values were computed from these latter curves by assuming an adiabatic relationship. The figures should be useful in estimating the time during the year that a specified environment might be expected.

The fourth and a very important quantity of interest is how the plasma parameters vary with time during a charging event. The approaches to determining this quantity range from detailed models of the magnetosphere to averages over many geomagnetic storms. For design purposes we have adopted a simulation of the electron and proton current and temperature that approximates natural variations in the potential as predicted by charging analysis codes (e.g., NASCAP). A time variation sequence suitable for modeling the worst effects of a geomagnetic storm is recommended (fig. 15). (Note that the simple single-Maxwellian representation has been found to match flight data when used in NASCAP studies.)

Derivation of Moments of Plasma Distribution Function

The Earth's plasma can be described, as discussed earlier, in terms of simple Maxwell-Boltzmann distributions. As this representation lends itself to efficient manipulation when carrying out charging calculations, it is often the preferred way for describing plasmas. The Maxwell-Boltzmann distribution F_i is given by

$$F_i(v) = n_i \left(\frac{m_i}{2\pi k T_i} \right)^{3/2} \exp\left(\frac{-m_i v^2}{2kT_i} \right) \qquad \text{(A1)}$$

where

n_i number density of species i

m_i mass of species i

k Boltzmann constant

T_i temperature of species i

TABLE IX. - WORST-CASE GEOSYNCHRONOUS ENVIRONMENTS

[The moments T_{av} and T_{rms} are averaged over all angles. The SCATHA two-Maxwellian parameters are for fluxes parallel and perpendicular to the magnetic field. ATS-6 two-Maxwellian parameters are averaged over all directions.]

Parameter	Source					
	Deutsch (1981)		Mullen et al. (1981)		Mullen and Gussenhoven (1982)	
	Date					
	Day 178, 1974		Day 114, 1979		———	
	Spacecraft					
	ATS-6		SCATHA		SCATHA	
	Electrons	Ions	Electrons	Ions	Electrons	Ions
Number density, ⟨ND⟩, cm^{-3}	1.12	0.245	0.900	2.30	3.00	3.00
Current density, ⟨J⟩, nA cm^{-2}	0.410	0.0252	0.187	0.795×10^{-2}	0.501	0.0159
Energy denisty, ⟨ED⟩, eV cm^{-3}	0.293×10^{5}	0.104×10^{5}	0.960×10^{4}	0.190×10^{5}	0.240×10^{5}	0.370×10^{5}
Energy flux, ⟨EF⟩, eV cm^{-2} s^{-1} sr^{-1}	0.264×10^{14}	0.298×10^{12}	0.668×10^{13}	0.430×10^{13}	0.151×10^{14}	0.748×10^{12}
Number density for population 1, N_1, cm^{-3}:						
Parallel	———	0.882×10^{-2}	0.200	1.60	1.00	1.10
Perpendicular	———	———	0.200	1.10	0.800	0.900
Temperature for population 1, T_1, eV:						
Parallel	———	0.111×10^{3}	0.400×10^{3}	0.300×10^{3}	0.600×10^{3}	0.400×10^{3}
Perpendicular	———	———	0.400×10^{3}	0.300×10^{3}	0.600×10^{3}	0.300×10^{3}
Number density for population 2, N_2, cm^{-3}:						
Parallel	1.22	0.236	0.600	0.600	1.40	1.70
Perpendicular	———	———	2.30	1.30	1.90	1.60
Temperature for population 2, T_2, eV:						
Parallel	0.160×10^{5}	0.295×10^{5}	0.240×10^{5}	0.260×10^{5}	0.251×10^{5}	0.247×10^{5}
Perpendicular	———	———	0.248×10^{5}	0.282×10^{5}	0.261×10^{5}	0.256×10^{5}
Average temperature, T_{av}, eV	0.160×10^{5}	0.284×10^{5}	0.770×10^{4}	0.550×10^{4}	0.533×10^{4}	0.822×10^{4}
Root-mean-square temperature, T_{rms}, eV	0.161×10^{5}	0.295×10^{5}	0.900×10^{4}	0.140×10^{5}	0.733×10^{4}	0.118×10^{5}

v velocity

F_i distribution function of species i

Unfortunately, the space plasma environment is seldom a Maxwell-Boltzmann distribution. However, given the actual plasma distribution function, it is possible to define (irrespective of whether the plasma is Maxwell-Boltzmann or not) moments of the distribution function that reveal characteristics of its shape. These moments can in most cases then be used to determine an approximate Maxwell-Boltzmann distribution. The first four of these moments are

$$\langle ND_i \rangle = 4\pi \int_0^\infty (v^0) F_i v^2 dv \tag{A2}$$

$$\langle NF_i \rangle = \int_0^\infty (v^1) F_i v^2 dv \tag{A3}$$

$$\langle ED_i \rangle = \frac{4\pi m_i}{2} \int_0^\infty (v^2) F_i v^2 dv \tag{A4}$$

$$\langle EF_i \rangle = \frac{m_i}{2} \int_0^\infty (v^3) F_i v^2 dv \tag{A5}$$

where

$\langle ND_i \rangle$ first moment that equals n_i

$\langle NF_i \rangle$ number flux of species i

$\langle ED_i \rangle$ energy density of species i

$\langle EF_i \rangle$ energy flux of species i

For the Maxwell-Boltzmann distribution of equation (A1) these assume the following values:

$$\langle ND_i \rangle = n_i \tag{A6}$$

$$\langle NF_i \rangle = \left(\frac{n_i}{2\pi}\right) \left(\frac{2kT_i}{\pi m_i}\right)^{1/2} \tag{A7}$$

$$\langle ED_i \rangle = \frac{3}{2} n_i k T_i \tag{A8}$$

$$\langle EF_i \rangle = \left(\frac{m_i}{\pi}\right) \left(\frac{kT_i}{\pi m_i}\right)^{3/2} \tag{A9}$$

Often it is easier to measure the four moments of the plasma distribution function than the actual temperature. This is particularly true for space plasmas, where the concept of "temperature" is not well defined. As an

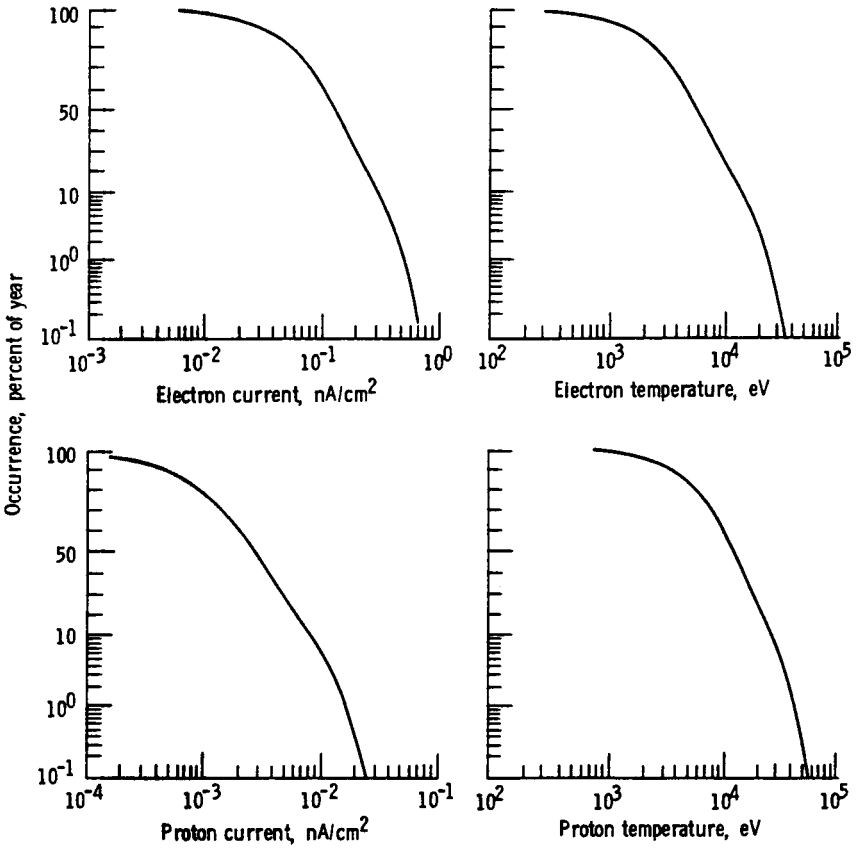

Figure 14.—Occurrence frequencies of plasma parameters.

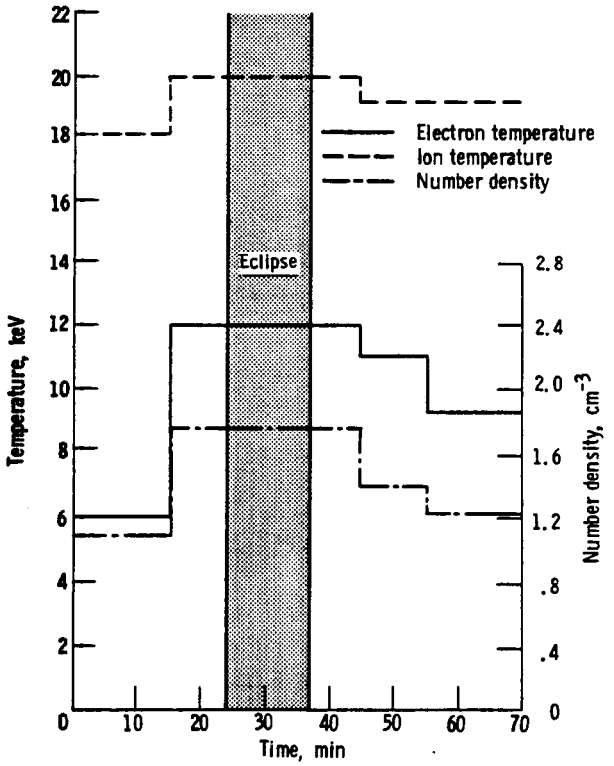

Figure 15.—Time history of model substorm.

illustration, from the four moments, two definitions of the plasma temperature can be developed:

$$T_{av} = \frac{2\langle ED \rangle}{3\langle ND \rangle} \tag{A10}$$

$$T_{rms} = \frac{\langle EF \rangle}{\langle NF \rangle} \tag{A11}$$

For a true Maxwell-Boltzmann plasma there quantities would be equal; for actual plasmas T_{rms} is usually greater than T_{av}. Even so, experience has shown that a representation in terms of two Maxwell-Boltzmann distributions is in fact a better mathematical representation of the space plasma than a single Maxwellian. That is, the plasma distribution for a single species can be represented by

$$F_2(v) = \left(\frac{m}{2\pi k}\right)^{3/2} \left[\left(\frac{N_1}{T_1^{3/2}}\right) \exp\left(\frac{-mv^2}{2kT_1}\right) + \left(\frac{N_2}{T_2^{3/2}}\right) \exp\left(\frac{-mv^2}{2kT_2}\right) \right] \tag{A12}$$

where

N_1 number density for population 1
T_1 temperature for population 1
N_2 number density for population 2
T_2 temperature for population 2

This representation in most cases fits the data quite adequately over the energy range of importance to spacecraft charging. Further, it is very simple to derive N_1, T_1, N_2, and T_2 directly from the four moments so that a consistent mathematical representation of the plasma can be established that incorporates the simplicity of the Maxwell-Boltzmann representation while maintaining a physically reasonable picture of the plasma. The distinction between T_{av}, T_{rms}, T_1, and T_2 must be kept in mind, however, whenever reference is made to a "Maxwell-Boltzmann" distribution as these are only approximations at best to the actual plasma environment.

Appendix B

Technical Description of NASCAP

The NASA Charging Analyzer Program (NASCAP) is a quasi-static computational program (i.e., it assumes that currents are functions of environmental parameters, electrostatic potentials, and magnetostatic fields but are not dependent on electrodynamic effects). This is reasonable since charging times in insulators are long compared with the computing interval. The following paragraphs briefly discuss the elements of NASCAP. Detailed descriptions (Katz et al., 1977, 1979, 1981), including a users manual (Cassidy, 1978), are available.

A flow diagram of NASCAP is shown in figure 16. The logic has been designed to provide maximum flexibility to the user. As execution progresses, the user may request a charging simulation or any of several auxiliary functions such as object definition, particle emitter, or detector simulation. NASCAP contains full restart capability.

A NASCAP charging simulation first calculates the currents incident on and emitted from all surfaces for a given environment. From these currents it computes the new electrostatic potentials (relative to the space plasma potential) on all spacecraft surfaces and in surrounding space. This iteration continues for a user-specified period of time. The charging simulation can take into account such effects as internal bias voltages, Debye screening, and charged-particle emitters.

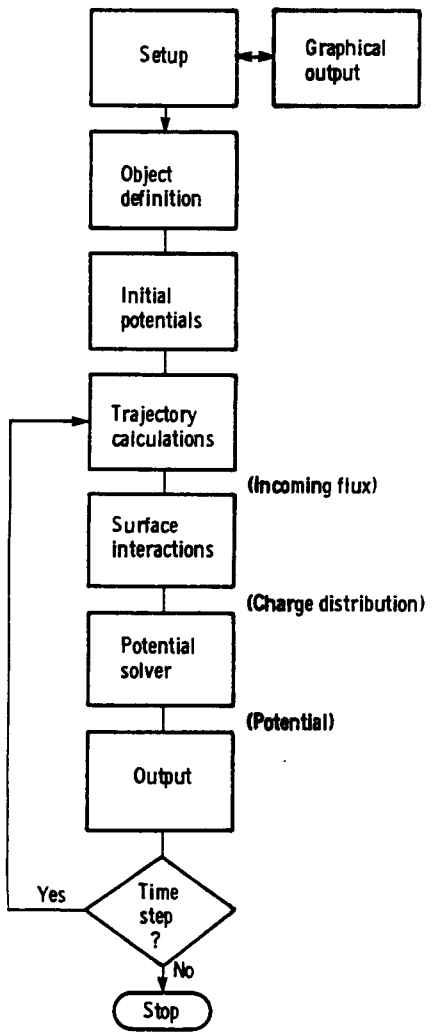

Figure 16.—Flow diagram of NASA Charging Analyzer Program (NASCAP).

Computational Space

NASCAP computations are performed in an embedded set of cubic grids of dimensions $17 \times 17 \times (4n+1)$, where $4 \leq n \leq 8$ (fig. 17). The object is described in the innermost grid. Each successive grid has twice the linear dimensions of the next inner one. This allows treatment of a large volume of space while minimizing computational time and storage.

Environment Definition

In NASCAP the charged-particle environment can be specified in a number of ways. For simulating space environments the most commonly used techniques are the Maxwellian and double-Maxwellian descriptions of geomagnetic substorms. These allow independent specification of temperatures and particle densities of both electron and proton components. Actual particle distributions from flight instruments can also be used to specify the space environment for both quiescent and substorm conditions. Anisotropic fluxes to various surfaces can also be defined.

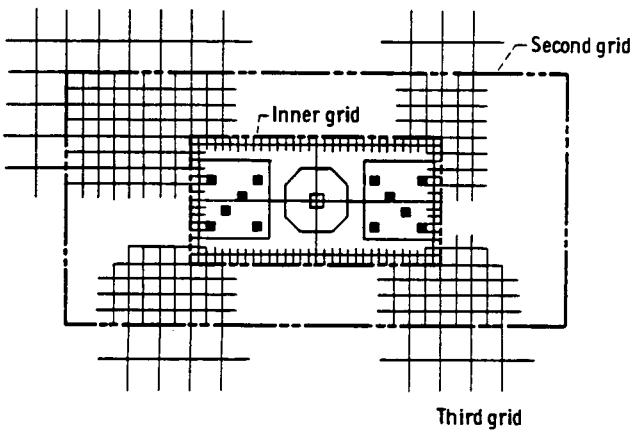

Figure 17.—NASCAP nested grid computational space.

NASCAP also treats surface charging in laboratory simulations. For these cases, single or multiple beams of electrons or ions can be specified from arbitrary locations. Since the surface charging physics is the same for both space and laboratory simulation environments, the accuracy of NASCAP predictions can be determined from laboratory results where environment fluxes can be controlled and detailed measurements made. The predictions are generally within 20 percent of the experimental surface voltages.

Object Definition

NASCAP requires that an object be defined in terms of thin booms, flat plates, rectangular parallelepipeds, or sections of parallelepipeds. Only thin booms extend beyond the innermost grid boundary. Furthermore, no other portion of the object must touch the innermost grid boundary. This object definition protocol allows rather complex spacecraft models to be defined by using fairly simple inputs.

Since a spacecraft can be a complex shape and errors in describing the model in terms of program limitations can arise, a graphical output of the spacecraft model can be generated by the computer to verify the accuracy of the model before start of computations. (See fig. 18 for an example of output.) Any set of axes or rotational angles can be specified for viewing the object. The graphical output of the object definition identifies the specified materials used on the surfaces. Hence, it is possible to determine that the computer model is the desired representation of the spacecraft.

Material Properties

NASCAP allows surfaces to be bare or covered with a thin ($\sim 10^{-4}$ m) dielectric material. Values of properties for common spacecraft materials (e.g., aluminum, gold, Teflon, Kapton, and silica) are supplied in the code and can be adjusted if desired by the user. Properties for other materials must be specified by the user. The properties required by NASCAP are dielectric constant, material thickness, backscatter and secondary emission coefficients (for both electron and proton impact), bulk and surface conductivities, photoemission yield, electrical breakdown thresholds, and radiation-induced conductivity properties.

Electrical Connectivity

In NASCAP the spacecraft model can be composed of up to 15 separate conductors. These conductors can be resistively or capacitively coupled and can be allowed to float, to be held at fixed potentials, or to be biased relative to one another. In the latter case, NASCAP automatically transports charge from one conductor to another to maintain the bias voltages.

Mathematical Algorithm

NASCAP uses an incomplete Cholesky conjugate gradient algorithm to calculate the change in spacecraft potential at each time step ($\sim 10^3$ variables). The spacecraft equivalent circuit used in this calculation is set up by geometrical analysis within NASCAP. The potential in the external space ($\sim 10^4$ to 10^5 variables) is calculated by a finite-element, sealed-conjugate-gradient technique. Both potential solvers are capable of handling mixtures of fixed-potential and fixed-charge boundary conditions at the spacecraft surface.

Detectors

At any time interval after the charging simulation begins, the user can request a simulation of a particle detector behavior. The user specifies the location of a detector, an aperture, and a range of viewing angles or particle angles. NASCAP then computes particle

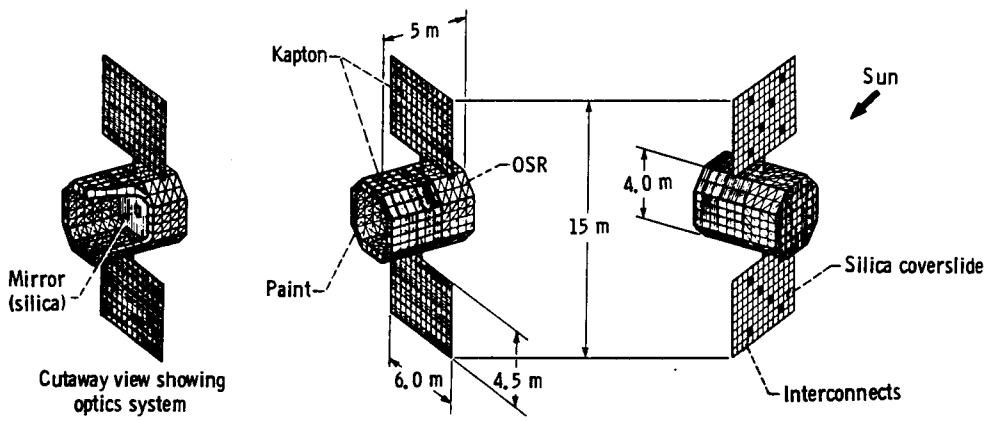

CS-80-594

Figure 18.— NASCAP model of large optics system satellite.

trajectories, by using predicted surface voltages and external fields, from the detector location to either emission from another part of the spacecraft or arrival from space. (See fig. 19.) Those particles arriving from space are assumed to be those that the particle detector should sense. Both electron and proton detectors can be specified.

Emitters

NASCAP can treat electron- or proton-emitting devices if they are designed to operate at low current densities (e.g., as active charge control devices on geosynchronous spacecraft). This limitation is imposed because NASCAP does not take into account the formation of space charge barriers in front of the emitter. Space charge effects become significant for electron emission at currents greater than a few milliamperes and for proton emission at currents greater than 0.1 mA.

The user specifies the emitter location, the current density and energy, and the beam direction and spread. NASCAP traces these particles to either the computational boundary (where they are considered to be lost) or to another spacecraft surface. The total emitter current is considered to be a loss of charge (either positive or negative depending on the emitter) to the conductor associated with the emitter location. Particles that return to a spacecraft surface are considered to be a source of charge for that surface. Hence, both emission and collection of the particles are considered in computing the object potential.

Output

In addition to its standard printed output, NASCAP provides an extensive menu of graphical outputs and printed data compilations. Graphical output includes the material and perspective object definition pictures, potential contour plots, and particle trajectory plots. The standard printed output includes a summary of all cell voltages, listing of currents to specified surface cells, and compilation of electrical stress through insulators in decreasing order. Sorting routines can tabulate specific cell potentials as a function of time for specified sets of cell numbers or materials. Sufficient information is stored in external files to allow a restart of a NASCAP program for further analysis, for evaluation under changed environmental conditions, or for postprocessing analysis with user-written programs.

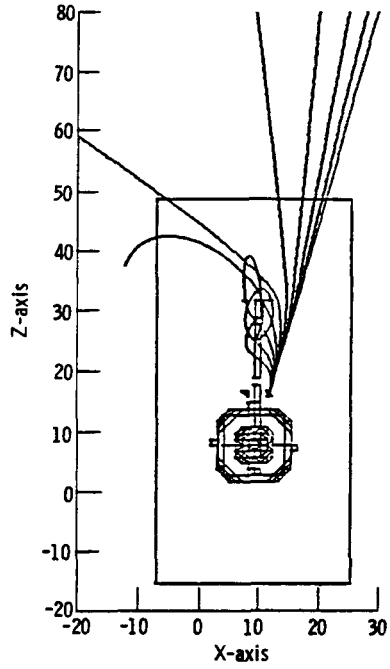

Figure 19.—Electron trajectories for Galileo (Harel et al., 1982).

Appendix C

Voyager SEMCAP Analysis

To simulate the effects of arc discharges on Voyager, either a high-voltage-excited spark gap or a flat-plate capacitor with an arc gap was used to induce arcs. The radiated fields from these sources were approximated in the Specification and Electomagnetic Compatibility Program (SEMCAP) in two ways:

(1) An induction field model consisting of quasi-static electric and magnetic fields proportional to the voltage and current of the source, respectively

(2) A radiated field model representing the far-field electromagnetic radiation of the loop antenna formed by the source

The Voyager test results using SEMCAP and these assumed arc source models are presented in table X along with the values actually observed. The source parameters used in the predictions are presented in table XI (reflecting the arc parameters of the test source). The mean error between the predicted and measured results is −6 dB, and the standard deviation is 23 dB. Assuming these accuracy parameters to be applicable to predicted in-flight responses for Voyager, the spacecraft was considered to be immune to arc discharges below 20 mV on the basis of the SEMCAP analysis. The use of SEMCAP in this application caused numerous design changes that significantly improved the arc discharge protection of the Voyager spacecraft. Even though flight Voyagers still suffered several arc discharge events, the design changes resulting from SEMCAP (in conjunction with testing) are believed to have significantly enhanced their survivability.

TABLE X. – SEMCAP PREDICTIONS

[Mean error, -12 dB (underpredicting); standard deviation, 20 dB – not including entries footnoted a.]

Location of arc	High gain antenna		Infrared interferometer/ spectrometer		OBLFM		Sun sensor	
	Predicted	Measured	Predicted	Measured	Predicted	Measured	Predicted	Measured
Voltage values from radiated tests								
Infrared interferometer/spectrometer (IRIS) imaging subsystem	0.9	1.2	2.0	0.8	0.09	1.0	0.08	2.5
Low-energy charged-particle experiment	1.5	.8	6.0	[a] .45	.4	.7	.1	1.6
Sun sensor	.84	1.0	.48	[a] .3	.9	[a] .4	4.0	1.6
Magnetometer	.4	[a] .4	.8	[a] .5	3.6	1.2	.4	.5
Frequency-selective subreflector	4.9	4.0	.96	1.5	2.1	1.4	.002	2.0
Brewster plate[b]	2.2	4.0	1.5	4.0	.9	3.3	.54	17.7
Voltage values from surface tests								
Low-energy charged-particle experiment	0.27	0.6	15	[a]0.6	0.04	0.6	0.017	0.8
Brewster plate	6.8	1.0	.37	.6	.6	.7	.4	.9
Frequency-selective subreflector	57	[c]10	.09	[c]4.2	.2	[a]1.7	.001	[a]4.0

[a]Background noise; noise due to arc unnoticeable.
[b]Predicted was "contact" test; measured was "radiated" test.
[c]Extrapolated.

TABLE XI. - IN-FLIGHT ARC MODELS - SEMCAP PREDICTIONS VERSUS ESD TEST RESULTS (FLIGHT SPACECRAFT)

[Parameters of in-flight arc models (after scaling test data to spacecraft dimensions).]

Arc source	Breakdown voltage, V, kV	Discharge or arc current, I, A	Discharge current risetime, t_r, ns	Discharge current pulse width, t_p, ns	Main discharge capacitance, C, nF	Energy, E, mJ
Magnetometer cable	5	20	10	1700	50	62.5
High-gain antenna paint (outboard)	1	150	5	3000	400	200
Plume shield (separation connector)	1	16	20	285	4.5	2.25
Frequency-selective subreflector	7	80	8	80	.014	.34
High-gain antenna paint (inboard)	1	150	5	2400	300	.15
Plume shield (radioisotope thermoelectric generator, RTG)	1	16	20	330	5.2	2.6
RTG oxide	3.5	925	20	3700	340	2080
Modified infrared interferometer/ spectrometer (MIRIS) Kapton	1	150	5	26	.04	.02
Brewster plate[a]	1	2	3	10	20	10.0
Separation connector	5	36	10	15	.15	1.88
Magnetometer Teflon[b]	1	3	5	13	.038	.02

[a]No area scaling needed because sample was entire item.
[b]Teflon models are believed to be well understood.

Bibliography

Spacecraft Charging Technology—1978. NASA CP-2071, 1979.

Spacecraft Charging Technology—1980, NASA CP-2182, 1981.

Adamo, R. C.; and Nanevicz, J. E.: Spacecraft-Charging Studies of Voltage Breakdown Processes on Spacecraft Thermal Control Mirrors. Spacecraft Charging by Magnetospheric Plasmas, A. Rosen, ed., Prog. Astronaut. Aeronaut., vol. 47, MIT Press, 1976, 225-235.

Al' Pert, I. L.: Wave-Like Phenomena in the Near-Earth Plasma and Interactions with Man-Made Bodies. *Geophysics III*, Part V, K. Rawer, ed., Springer-Verlag, 1976, pp. 217-349.

Aron, P. R.; and Staskus, J. V.: Area Scaling Investigations of Charging Phenomena. Spacecraft Charging Technology—1978, NASA CP-2071, 1979, pp. 485-506.

Balmain, K. G.: Surface Discharge Effects—Induced Electric Arcs from Spacecraft Dielectric Sheets. Space Systems and Their Interactions with Earth's Space Environment. H. B. Garrett and C. P. Pike, eds., Prog. Astronaut. Aeronaut., vol. 71, AIAA, 1980, pp. 276-298.

Balmain, K. G.: Scaling Laws and Edge Effects for Polymer Surface Discharges. Spacecraft Charging Technology—1978, NASA CP-2071, 1979, pp. 646-656.

Balmain, K. G.: Surface Discharge Arc Propagation and Damage on Spacecraft Dielectrics. Spacecraft Materials in Space Environment—Conference Proceedings, J. Dauphin and T. D. Guyenne, eds., European Space Agency, 1979, pp. 209-215.

Balmain, K. G.; Cuchanski, M.; and Kremer, P. C.: Surface Micro-Discharges on Spacecraft Dielectrics. Proceedings of the Spacecraft Charging Technology Conference, C. P. Pike and R. R. Lovell, eds., NASA TM X-73537, 1977, pp. 519-526.

Balmain, K. G; and Dubois, G. R.: Surface Discharges on Teflon, Mylar, and Kapton. IEEE Trans. Nucl. Sci., vol. NS-26, Dec. 1979, pp. 5146-5151.

Balmain, K. G.; and Hirt, W.; Dielectric Surface Discharges: Dependence on Incident Electron Flux. IEEE Trans. Nucl. Sci., vol. NS-27, no. 6, Dec. 1980, pp. 1770-1775.

Balmain, K. G.; Orszag, M.; and Kremer, P.: Surface Discharges on Spacecraft Dielectrics in a Scanning Electron Microscope. Spacecraft-Charging by Magnetospheric Plasmas, A. Rosen, ed., Prog. in Astronaut. Aeronaut. vol. 47, MIT Press, 1976, pp. 213-223.

Baragiola, R. A.; Alonso, E. V.; and Florio, A. O.: Electron Emission from Clean Metal Surfaces Induced by Low-Energy Light Ions. Phys. Rev. B., vol. 19, no. 1, Jan. 1, 1979, pp. 121-129.

Bartlett, R. O.; DeForest, S. E.; and Goldstein, P.: Spacecraft Charging Control Demonstration at Geosynchronous Altitude, AIAA Paper 75-359, Mar. 1975.

Bartlett, R. O.; and Purvis, C. K.: Summary of the Two-Year NASA Program for Active Control of ATS-5/6 Environmental Charging. Spacecraft Charging Technology—1978, NASA CP-2071, 1979, pp. 44-58.

Beattie, J. R.; and Goldstein, R.: Active Spacecraft Potential Control System Selection for the Jupiter Orbiter with Probe Mission. Proceedings of the Spacecraft Charging Technology Conference, C. P. Pike and R. R. Lovell, eds., NASA TM X-73537, 1977, pp. 143-166.

Beers, B. L.; Pine, V. W.; and Ives, S. T.: Continued Development of a Detailed Model of Arc Discharge Dynamics. (BEERS 1-82-16-23, Beers Associates; NASA Contract NAS3-22530.) NASA CR-167977, 1982.

Beers, B. L.; Pine, V. W.; and Ives, S. T.: Internal Breakdown of Charged Spacecraft Dielectrics. IEEE Trans. Nucl. Sci., vol. NS-28, Dec. 1981, pp. 4529-4534.

Beers, B. L.; Pine, V. W.; and Ives, S. T.: Theoretical Properties of Streamers in Solid Dielectrics. 1981 Annual Report. Conference on Electrical Insulation and Dielectric Phenomena. IEEE, 1981, pp. 390-397.

Beers, B. L.; et al.: First Principles Numerical Model of Avalanche-Induced Arc Discharges in Electron-Irradiated Dielectrics. (SAI-102-79-002, Science Applications, NASA Contract NAS3-21378.) NASA CR-159560, 1979.

Belanger, V. J.; and Eagles, A. E.: Secondary Emission Conductivity of High Purity Silica Fabric. Proceedings of the Spacecraft Charging Technology Conference, C. P. Pike and R. R. Lovell, NASA TM X-73537. 1977, pp. 655-686.

Berkopec, F. D.; Stevens, N. J.; and Sturman, J. C.: The Lewis Research Center Geomagnetic Substorm Simulation Facility. Proceedings of the Spacecraft Charging Technology Conference, C. P. Pike, and R. R. Lovell, eds., NASA TM X-73537, 1977, pp. 423-430.

Bernstein, I. B.; and Rabinowitz, I. N.: Theory of Electrostatic Probes in a Low-Density Plasma. Phys. Fluids, vol. 2, no. 2, Mar.-Apr. 1959, pp. 112-121.

Besse, A. L.: Unstable Potential of Geosynchronous Spacecraft. J. Geophys. Res., vol. 86, Apr. 1, 1981, pp. 2443-2446.

Besse, A. L.; and Rubin, A. G.: A Simple Analysis of Spacecraft Charging Involving Blocked Photoelectrons. J. Geophys. Res., vol. 85, May 1, 1980, pp. 2324-2328.

Bever, R. S.; and Staskus, J.: Tank Testing of a 2500-cm^2 Solar Panel. Spacecraft Charging Technology—1980, NASA CP-2182, 1981, pp. 211-227.

Bower, S. P.: Spacecraft Charging Characteristics and Protection. IEEE Trans. Nucl. Sci., vol. NS-24, Dec. 1977, pp. 2266-2269.

Cassidy, J. J., III: NASCAP User's Manual—1978 (SSS-R-78-3739, Systems Science and Software; NASA Contract NAS3-21050.) NASA CR-159417, 1978.

Cauffman, D. P.: Ionization and Attraction of Neutral Molecules to a Charged Spacecraft. Report SD-TR-80-78, Aerospace Corp., 1980. (AD-A093287.)

Cauffman, D. P.: The Effects of Photoelectron Emission on a Multiple-Probe Spacecraft near the Plasmapause. Photon and Particle Interactions with Surfaces in Space, R. J. L. Grard, ed., D. Reidel Publ. Co., 1973, pp. 153-161.

Chase, R. W.: Secondary Electron Emission Yield from Aluminum Alloy Surfaces. Ph. D. Thesis, Case Western Reserve Univ., 1979.

Chen, F. F.: Electric Probes. Plasma Diagnostic Techniques, R. H. Huddlestone and S. L. Leonard, eds., Academic Press, 1965, pp. 113-200.

Chung, M. S.; and Everhart, T. E.: Simple Calculation of Energy Distribution of Low-Energy Secondary Electrons Emitted from Metals Under Electron Bombardment. J. Appl. Phys., vol. 45, no. 2, Feb. 1974, pp. 707-709.

Cipolla, J. W. Jr.; and Silevitch, M. B.: Analytical Study of the Time Dependent Spacecraft-Plasma Interaction. Spacecraft Charging Technology—1978, NASA CP-2071, 1979, pp. 197-208.

Clark, D. M.; and Hall, D. F.: Flight Evidence of Spacecraft Surface Contamination Rate Enhancement by Spacecraft Charging Obtained with a Quartz Crystal Microbalance. Spacecraft Charging Technology, NASA CP-2182, 1981, pp. 493-508.

Coakley, P.; Kitterer, B.; and Treadaway, M.: Charging and Discharging Characteristics of Dielectric Material Exposed to Low- and Mid-Energy Electrons. IEEE Trans. Nucl. Sci., vol. NS-29, Dec. 1982, pp. 1639-1643.

Coakley, P. G.; Wild, N.; and Treadaway, M. J.: Laboratory Investigation of Dielectric Materials Exposed to Spectral Electron Environments (1 to 100 keV). IEEE Trans. Nucl. Sci., vol. NS-30, Dec. 1983, pp. 4605-4609.

Cohen, H. A.; et al.: Design, Development, and Flight of a Spacecraft Charging Sounding Rocket Payload. Spacecraft Charging Technology—1978, NASA CP-2071, 1979, pp. 80-90.

Darlington, E. H.; and Cosslett, V. E.: Backscattering of 0.5-10 keV Electrons from Solid Targets, J. Phys. D., vol. 5, no. 11, Nov. 1972, pp. 1969-1981.

DeForest, S. E.: Electrostatic Potentials Developed by ATS-5. Photon and Particle Interactions with Surfaces in Space, R. J. L. Grard, ed., D. Reidel Publ. Co., 1973, pp. 263-276.

DeForest, S. E.: Spacecraft Charging at Synchronous Orbit. J. Geophys. Res., vol. 77, Feb. 1, 1972, pp. 651-659.

DeForest, S. E.; and Goldstein, R.: A Study of Electrostatic Charging of ATS-5 During Ion Thruster Operation. (JPL-953675, Jet Propulsion Lab.; NASA Contract NAS7-100.) NASA CR-145910, 1973.

DeForest, S. E.; and McIlwain, C. E.: Plasma Clouds in the Magnetosphere. J. Geophys. Res., vol. 76, June 1, 1971, pp. 3587-3611.

Dekker, A. J.: Secondary Electron Emission. Solid State Physics, Advances in Research and Applications, vol. 6, Academic Press, 1958, pp. 251-311.

Durrett, J. C.; and Stevens, J. R.: Description of the Space Test Program P78-2 Spacecraft and Payloads. Spacecraft Charging Technology—1978, NASA CP-2071, 1979, pp. 4-10.

Evdokimov, O. B.; and Tubalov, N. P.: Stratification of Space Charge in Dielectrics Irradiated with Fast Electrons. Sov. Phys. Solid State, vol. 15, no. 9, Mar. 1974, pp. 1869-1870.

Fahleson, U.: Plasma-Vehicle Interactions in Space—Some Aspects on Present Knowledge and Future Development. Photon and Particle Interactions with Surfaces in Space, R. J. L. Grard, ed., D. Reidel Publ. Co., 1973, pp. 563-569.

Fellas, C. N.; and Richardson, S.: Internal Charging of Indium Oxide Coated Mirrors. IEEE Trans. Nucl. Sci., vol. NS-28, Dec. 1981, pp. 4523-4528.

Fennel, J. F.; et al.: A Review of SCATHA Satellite Results: Charging and Discharging. Spacecraft/Plasma Interactions and Their Influence on Field and Particle Measurements, A. Pedersen, T. D. Guyenne, and J. Hunt, eds., European Space Agency, ESA-SP-198, 1983, pp. 3-11.

Feuerbacher, B.; Willis, R. F.; and Fitton, B.: Electrostatic Charging and Formation of Composite Interstellar Grains. Photon and Particle Interactions with Surfaces in Space, R. J. L. Grard, ed., D. Reidel Publ. Co., 1973, pp. 415-426.

Fredricks, R. W.; and Scarf, F. L.: Observations of Spacecraft Charging Effects in Energetic Plasma Regions. Photon and Particle Interactions with Surfaces in Space, R. J. L. Grard, ed., D. Reidel Publ. Co., 1973, pp. 277-308.

Fredrickson, A. R.: Bulk Charging and Breakdown in Electron-Irradiated Polymers. Spacecraft Charging Technology—1980, NASA CP-2182, 1981, pp. 33-51.

Fredrickson, A. R.: Radiation Induced Dielectric Charging. Space Systems and Their Interactions with the Earth's Space Environment, H. B. Garrett and C. P. Pike, eds., Prog. Astronaut. Aeronaut., vol. 71, AIAA, 1980, pp. 386-412.

Fredrickson, A. R.: Electric Fields in Irradiated Dielectrics. Spacecraft Charging Technology—1978, NASA CP-2071, 1979, pp. 554-569.

Garrett, H. B.: The Charging of Spacecraft Surfaces. Rev. Geophys., vol. 19, Nov. 1981, pp. 577-616.

Garrett, H. B.: Review of Quantitative Models of the 0 to 100 keV Near-Earth Plasma, Rev. Geophys. Space Phys., vol. 17, no. 3, 1979, pp. 397-417.

Garrett, H. B.: Modeling of the Geosynchronous Plasma Environment. Spacecraft Charging Technology—1978, NASA CP-2071, 1979, pp. 11-22.

Garrett, H. B.; Schwank, D. C.; and DeForest, S. E.: A Statistical Analysis of the Low-Energy Geosynchronous Plasma Environment—I. Electrons. Planet Space Sci., vol. 29, Oct. 1981, pp. 1021-1044.

Garrett, H. B.; and Pike, C. P., eds., Space Systems and Their Interactions with Earth's Space Environment. Prog. Astronaut. Aeronaut., vol. 71, AIAA, 1980.

Garrett, H. B.; and DeForest, S. E.: Time-Varying Photoelectron Flux Effects on Spacecraft Potential at Geosynchronous Orbit. J. Geophys. Res., vol. 84, May 1, 1979, pp. 2083-2088.

Garrett, H. B.; and DeForest, S. E.: An Analytical Simulation of the Geosynchronous Plasma Environment. Planet. Space Sci., vol. 27, Aug. 1979, pp. 1101-1109.

Garrett, H. B.; et al.: Modeling of the Geosynchronous Orbit Plasma Environment—Part 2. ATS-5 and ATS-6 Statistical Atlas. AFGL-TR-78-0304, Air Force Geophysics Lab., 1978. (AD-A067018.)

Garrett, H. B.; Pavel, A. L.; and Hardy, D. A.: Rapid Variations in Spacecraft Potential. AFGL-TR-77-0132, Air Force Geophysics Lab., 1977. (AD-A046350.)

Garrett, H. B.; and Rubin, A. G.: Spacecraft Charging at Geosynchronous Orbit—Generalized Solution for Eclipse Passage. Geophys. Res. Lett., vol. 5, Oct. 1978, pp. 865-868.

Garrett, H. B.; Rubin, A. G.; and Pike, C. P.: Prediction of Spacecraft Potentials at Geosynchronous Orbit. Solar-Terrestrial Predictions Proceedings, Vol. II, R. F. Donnelly, ed., NASA TM-81061, 1979, pp. 104-118.

Gibbons, D. J.: Secondary Electron Emission. Handbook of Vacuum Physics, vol. 2, Pts. 2 and 3, A. H. Beck, ed., Pergamon Press, 1966, pp. 301-395.

Goldstein, R.: Active Control of Potential of the Geosynchronous Satellites ATS-5 and ATS-6. Proceedings of the Spacecraft Charging Technology Conference, C. P. Pike and R. R. Lovell, eds., NASA TM X-73537, 1977, pp. 121-129.

Goldstein, R.; and DeForest, S. E.: Active Control of Spacecraft Potentials at Geosynchronous Orbit. Spacecraft Charging by Magnetospheric Plasmas, A. Rosen, ed., Prog. Astronaut. Aeronaut., vol. 47, MIT Press, 1976, pp. 169-181.

Gonfalone, A.; et al.: Spacecraft Potential Control on ISEE-1. Spacecraft Charging Technology—1978, NASA CP-2071, 1979, pp. 256-267.

Gore, J. V.: The Design, Construction, and Testing of the Communications Technology Satellite Protection Against Spacecraft Charging. Proceeding of the Spacecraft Charging Technology Conference, C. P. Pike, and R. R. Lovell, eds., NASA TM X-73537, 1977, pp. 773-788.

Grard, R. J. L.: The Multiple Applications of Electrons in Space. Proceedings of the Spacecraft Charging Technology Conference, C. P. Pike and R. R. Lovell, eds., NASA TM X-73537, 1977, pp. 203-221.

Grard, R. J. L.: Spacecraft Potential Control and Plasma Diagnostic Using Electron Field Emission Probes. Space Sci. Instrum., vol. 1, Aug. 1975, pp. 363-376.

Grard, R. J. L., ed.: Photon and Particle Interactions with Surface in Space, D. Reidel Publ. Co., 1973.

Grard, R. J. L.: Properties of the Satellite Photoelectron Sheath Derived from Photoemission Laboratory Measurements. J. Geophys. Res., vol. 78, June 1, 1973, pp. 2885–2906.

Grard, R. J. L.; DeForest, S. E.; and Whipple, E. C., Jr.: Comment on Low Energy Electron Measurements in the Jovian Magnetosphere. Geophys. Res. Lett., vol. 4, June 1977, pp. 247–248.

Grard, R. J. L.; Knott, K.; and Pedersen, M. R.: Spacecraft Charging Effects. Space Sci. Rev., vol. 34, Mar. 1983, pp. 289–304.

Grard, R. J. L.; Knott, K.; and Pedersen, A.: Influence of Photoelectron and Secondary Emission on Electric Field Measurements in the Magnetosphere and Solar Wind. Photon and Particle Interactions with Surfaces in Space, R. J. L. Grard, ed., D. Reidel Publ. Co., 1973, pp. 163–189.

Grard, R. J. L.; and Tunaley, J. K. E.: Photoelectron Sheath Wear—a Planar Probe in Interplanetary Space. J. Geophys. Res., vol. 76, Apr. 1971, pp. 2498–2505.

Gross, B.; and Nablo, S. V.: High Potentials in Electron-Irradiated Dielectrics. J. App. Phys., vol. 38, no. 5, Apr. 1967, pp. 2272–2275.

Guernsey, R. L.; and Fu, J. H. M.: Potential Distributions Surrounding a Photo-Emitting Plate in a Dilute Plasma. J. Geophys. Res., vol. 75, June 1, 1970, pp. 3193–3199.

Gussenhoven, M. S.; and Mullen, E. G.: A "Worst Case" Spacecraft Charging Environment as Observed by SCATHA on 24 April 1979. AIAA Paper 82-0271, Jan. 1982.

Hachenberg, O.; and Brauer, W.: Secondary Electron Emission from Solids. Adv. Electron. Electron Phys., L. Marton, ed., vol. 11, Academic Press, New York, 1959, pp. 413–499.

Hoffmaster, D. K.; and Sellen, J. M., Jr.: Spacecraft Material Response to Geosynchronous Substorm Conditions. Spacecraft Charging by Magnetospheric Plasmas, A. Rosen, ed., Prog. Astronaut. Aeronaut, vol. 47, MIT Press, 1976, pp. 185–211.

Hoge, D. G.: METEOSAT Spacecraft Charging Investigation. Spacecraft Charging Technology—1980, NASA CP-2182, 1981, pp. 814–834.

Inouye, George T.: Implications of Arcing due to Spacecraft Charging on Spacecraft EMI Margins of Immunity. (TRW-36186-6016-UE-00, TRW Defense and Space Systems Group; NASA Contract NAS3-21961.) NASA CR-165442, 1981.

Inouye, G. T.; et al.: Thermal Blanket Metallic Film Groundstrap and Second Surface Mirror Vulnerability to Arc Discharges. Spacecraft Charging Technology—1978, NASA CP-2071, 1979, pp. 657–682.

Inouye, G. T.: Spacecraft Potentials in a Substorm Environment. Spacecraft Charging by Magnetospheric Plasmas, A. Rosen, ed., Prog. Astronaut. Aeronaut., vol. 47, MIT Press, 1976, pp. 103–120.

Inouye, G. T.; and Sellen, J. M.: TDRSS Solar Array Arc Discharge Tests. Spacecraft Charging Technology—1978, NASA CP-2071, 1979, pp. 834–852.

Inouye, G. T.; and Sellen, J. M., Jr.: TDRSS Solar Array Design Guidelines for Immunity to Geomagnetic Substorm Charging Effects. Photovoltaic Specialists Conference, 13th Conference Record, IEEE, 1978, pp. 309–312.

Inouye, G. T.; and Sellen, J. M., Jr.: A Proposed Mechanism for the Initiation and Propagation of Dielectric Surface Discharges. Presented at the Symposium on the Effects of the Ionosphere on Space and Terrestrial Systems, (Arlington, Va.), Jan. 24–26, 1978.

Jemiola, J. M.; Spacecraft Contamination: A Review. Space Systems and Their Interactions with Earth's Space Environment, H. B. Garrett and C. P. Pike, eds., Prog. Astronaut. Aeronaut., vol. 71, MIT Press, 1980, pp. 680–706.

Jemiola, J. M.: Proceedings of the USAF/NASA International Spacecraft Contamination Conference, NASA CP-2039, 1978.

Johnson, B.; Quinn, J.; and DeForest, S. E.: Spacecraft Charging on ATS-6. Presented at the Symposium on Effects of the Ionosphere on Space and Terrestrial Systems, (Arlington, Va.), Jan. 24–26, 1978.

Johnson, R. G.: Review of Hot Plasma Composition Near Geosynchronous Altitude. Spacecraft Charging Technology—1980, NASA CP-2182, 1981, pp. 412–432.

Kamen, R. E.; et al.: Design Guidelines for Control of Spacecraft Charging. Spacecraft Charging Technology—1978, NASA CP-2071, 1979, pp. 817–818.

Kasha, M. A.: The Ionosphere and Its Interaction with Satellites. Gordon and Breach, 1969.

Katz, I.; et al.: NASCAP Simulations of Spacecraft Charging of the SCATHA Satellite. Spacecraft/Plasma Interactions and Their Influence on Field and Particle Measurements, A. Pedersen, D. Guyenne, and J. Hunt, eds., European Space Agency, 1983, pp. 109–114.

Katz, I.; Additional Application of the NASCAP Code—Vol. 1: NASCAP Extension. (SSS-R-81-4847, vol. 1, Systems Science and Software; NASA Contract NAS3-21762.) NASA CR-165349, 1981.

Katz, I.; et al.: A Theory of Dielectric Surface Discharges. IEEE Trans. Nucl. Sci., vol. NS-27, Dec. 1980, pp. 1786–1791.

Katz, I.; et al.: The Capabilities of the NASA Charging Analyzer Program, Spacecraft Charging Technology—1978, NASA CP-2071, 1979, pp. 101–122.

Katz, I.; et al.: Extension, Validation, and Application of the NASCAP Code. (SSS-R-79-3904, Systems Science and Software; NASA Contract NAS 3-21050.) NASA CR-159595, 1979.

Katz, I.; et al.: A Three Dimensional Dynamic Study of Electrostatic Charging in Materials. (SSS-R-77-3367, Systems Science and Software; NASA Contract NAS3-20119.) NASA CR-135256, 1977.

Katz, I.; et al.: NASCAP, A Three Dimensional Charging Analyzer Program for Complex Spacecraft, IEEE Trans. Nucl. Sci., vol. NS-24, Dec. 1977, pp. 2276–2280.

Katz, I.; et al.: Dynamic Modeling of Spacecraft in a Collisionless Plasma. Proceedings of the Spacecraft Charging Technology Conference, C. P. Pike and R. R. Lovell, eds., NASA TM X-73537, pp. 319–330, 1977.

Kerslake, W. R.; Goldman, R. G.; and Nieberding, W. C.; SERT II: Mission, Thruster Performance, and In-Flight Thrust Measurements. J. Spacecr. Rockets, vol. 8, Mar. 1971, pp. 213–224.

Kerslake, W. R.; and Ignaczak, L. R.: SERT II 1979 Extended Flight Thruster System Performance. AIAA Paper 79-2063, Oct. 1979.

Keyser, R. C.; et al.: Electron Induced Discharge Modelling, Testing, and Analysis for SCATHA, Vol. I. IRT-8161-5-1, IRT Corp., 1978. (AD-A095962.)

Knott, K.: The Equilibrium Potential of a Magnetospheric Satellite in an Eclipse Situation. Planet. Space Sci., vol. 20, Aug. 1972, pp. 1137–1146.

Komatsu, G. K.; and Sellen, J. M., Jr.: A Plasma Bridge Neutralizer for the Neutralization of Differentially Charged Surfaces. Effect of the Ionosphere on Space and Terrestrial Systems, J. Goodman, ed., U.S. Government Printing Office, 1978, pp. 317–321.

Koons, H. C.: Aspect Dependence and Frequency Spectrum of Electrical Discharges on the P78-2 (SCATHA) Satellite. Spacecraft Charging Technology—1980, NASA CP-2182, 1981, pp. 478–492.

Koons, H. C.: Characteristics of Electrical Discharges on the P78-2 Satellite (SCATHA). AIAA Paper 80-0333, Jan. 1980.

Krainsky, I.; et al.: Secondary Electron Emission Yields. Spacecraft Charging Technology—1980, NASA CP-2182, 1981, pp. 179–197.

Labreton, J. P.: Active Control of the Potential of ISEE-1 by an Electron Gun. Spacecraft/Plasma Interactions and Their Influence on Field and Particle Measurements, A. Pedersen, D. Guyenne, and J. Hunt, eds., European Space Agency, 1983, pp. 191–197.

Laframboise, J. G.; Kamitsuma M.; and Goddard, R.: Multiple Floating Potentials, Threshold-Temperature Effects and Barrier Effects in High-Voltage Charging of Exposed Surfaces on Spacecraft.

Spacecraft Materials in Space Environment, European Space Agency, 1982, pp. 269-275.

Laframboise, J. G.: Theory of Spherical and Cylindrical Langmuir Probes in a Collisionless Maxwellian Plasma at Rest, UTIAS-100, Univ. Toronto, 1966.

Laframboise, J. G.; Goddard, R. and Prokopenko, S. M. L.; Numerical Calculations of High-Altitude Differential Charging: Preliminary Results. Spacecraft Charging Technology—1978, NASA CP-2071, 1979, pp. 188-196.

Laframboise, J. G.; and Prokopenko, S. M. L.: Predictions of High-Voltage Differential Charging on Geostationary Spacecraft. Effect of the Ionosphere on Space and Terrestrial Systems, J. M. Goodman, ed., Naval Research Lab., 1978, pp. 293-301.

Laframboise, J. G.; and Prokopenko, S. M. L.: Numerical Simulation of Spacecraft Charging Phenomena. Proceedings of the Spacecraft Charging Technology Conference, C. P. Pike and R. R. Lovell, eds., NASA TM X-73537, 1977, pp. 309-318.

Laframboise, J. G.; et al.: Results from a Two Dimensional Spacecraft-Charging Simulation and Comparison with a Surface Photocurrent Model. Spacecraft Charging Technology—1980, NASA CP-2182, 1981, pp. 709-716.

Leadon, R.; and Wilkenfeld, J.: Model for Breakdown Process in Dielectric Discharges. Spacecraft Charging Technology—1978, NASA CP-2071, 1979, pp. 704-710.

Leung, M. S.; Tueling, M. B.; and Schnauss, E. R.: Effects of Secondary Electron Emission on Charging. Spacecraft Charging Technology—1980, NASA CP-2182, 1981, pp. 163-178.

Lewis, R. O., Jr.: Viking and STP P78-2 Electrostatic Charging Designs and Testing. Proceedings of the Spacecraft Charging Technology Conference, C. P. Pike and R. R. Lovell, eds., NASA TM X-73537, 1977, pp. 753-772.

Lin, D. L.: Electron Multiplication in Solids. Phys. Rev. B, vol. 20, no. 12, Dec. 15, 1979, pp. 5238-5245.

Lin, D. L.; and Beers, B. L.: Stochastic Treatment of Electron Multiplication Without Scattering in Dielectrics. J. Appl. Phys., vol. 52, May 1981, pp. 3575-3578.

Lovell, R. R.; et al.: Spacecraft Charging Investigation: A Joint Research and Technology Program. Spacecraft Charging by Magnetospheric Plasmas, A. Rosen, ed., Prog. Astronaut. and Aeronaut., vol. 47, MIT Press, 1976, pp. 3-14.

Lucas, A. A.: Fundamental Processes in Particle and Photon Interactions with Surfaces. Photon and Particle Interations with Surfaces in Space, R. J. L. Grard, ed., D. Reidel Publ. Co., 1973, pp. 3-21.

Mandell, M. J.; Harvey, J. M.; and Katz, I.: NASCAP User's Manual, (SSS-R-77-3368, Systems Science and Software; NASA Contract NAS3-20119.) NASA CR-135259, 1977.

Mandell, M.; Katz, I.; and Parks, D. E.: NASCAP Simulation of Laboratory Charging Tests Using Multiple Electron Guns. IEEE Trans. Nucl. Sci., vol. NS-28, Dec. 1981, pp. 4568-4570.

Mandell, M. J.; et al.: The Decrease in Effective Photocurrents due to Saddle Points in Electrostatic Potentials Near Differentially Charged Spacecraft. IEEE Trans. Nucl. Sci., vol. NS-25, Dec. 1978, pp. 1313-1317.

Massaro, M. J.; Green, T.; and Ling, D.: A Charging Model for Three-Axis Stabilized Spacecraft. Proceedings of the Spacecraft Charging Conference, C. P. Pike and R. R. Lovell, eds., NASA TM X-73537, 1977, pp. 237-270.

Massaro, M. J.; and Ling, D.: Spacecraft Charging Results for the DSCS-III Satellite. Spacecraft Charging Technology—1978, NASA CP-2071, 1979, pp. 158-178.

Mauk, B. H.; and McIlwain, C. E.: ATS-6 UCSD Auroral Particles Experiment. IEEE Trans. Aerosp. Electron. Syst., vol. AES-11, Nov. 1975, pp. 1125-1130.

Mazzella, A.; Tobenfeld, E.; and Rubin, A. G.: AFSIM—An Air Force Satellite Interactions Model. AFGL-TR-79-0138, RDP, Inc., 1979. (AD-A078032.)

McIlwain, C. E.: Auroral Electron Beams Near the Magnetic Equator. Physics of the Hot Plasma in the Magnetosphere, B. Hultqvist and L. Stenflo, eds., Plenum, 1975, pp. 91-112.

McPherson, D. A.; and Schober, W.: Spacecraft Charging at High Altitudes: The SCATHA Satellite Program, Spacecraft Charging by Magnetospheric Plasmas, A. Rosen, ed., Prog. Astronaut. and Aeronaut., vol. 47, AIAA, 1976, pp. 15-30.

Meulenberg, A., Jr.: Evidence for a New Discharge Mechanism for Dielectrics in a Plasma. Spacecraft Charging by Magnetospheric Plasmas, A. Rosen, ed., Prog. Astronaut. Aeronaut., vol. 47, AIAA, 1976, pp. 237-246.

Mizera, P. F.: Natural and Artificial Charging—Results from the Satellite Surface Potential Monitor Flown on P78-2, AIAA Paper 80-0334, Jan. 1980.

Mizera, P. F.; et al.: Description and Charging Results from the SSPM. Spacecraft Charging Technology—1978, NASA CP-2071, 1979, pp. 91-100.

Mullen, E. G.; and Gussenhoven, M. G.: SCATHA Environmental Atlas, AFGL-TR-83-0002, Air Force Geophysics Lab., 1983. (AD-A131456.)

Nanevicz, J. E.; and Adamo, R. C.: Occurrence of Arcing and Its Effects in Space Systems. Space Systems and Their Interactions With Earth's Space Environment, H. B. Garrett and C. P. Pike, eds., AIAA Prog. Astronaut. Aeronaut., vol. 71, 1980, pp. 252-275.

Norman, K.; and Freeman, R. M.: Energy Distribution of Photoelectrons Emitted from a Surface on the OGO-5 Satellite and Measurements of Satellite Potential. Photon and Particle Interactions with Surfaces in Space, R. J. L. Grard, ed., D. Reidel Publ. Co., 1973, pp. 231-244.

O'Dwyer, J. J.; and Beers, B. L.: Thermal Breakdown in Dielectrics. 1981 Annual Report, Conference on Electrical Insulation and Dielectric Phenomena, IEEE, 1981, pp. 193-198.

Ogawa, H. S.; Cole, R. K.; and Sellen, J. M., Jr.: Factors in the Electrostatic Equilibration Between a Plasma Thrust Beam and the Ambient Space Plasma. AIAA Paper 70-1142, Aug. 1970.

Ogawa, H. S.; Cole, R. K.; and Sellen, J. M., Jr.: Measurements of Equilibration Potential Between a Plasma "Thrust" Beam and a Dilute "Space" Plasma. AIAA Paper 69-263, Mar. 1969.

Olsen, R. C.: A Threshold Effect for Spacecraft Charging, J. Geophys. Res. vol. 88, Jan. 1, 1983, pp. 493-499.

Olsen, R. C.: The Hidden Ion Population of the Magnetosphere. J. Geophys. Res., vol. 87, May 1, 1982, pp. 3481-3488.

Olsen, R. C.: Operation of the ATS-6 Ion Engine and Plasma Bridge Neutralizer at Geosynchronous Altitude. AIAA Paper 78-663, Apr. 1978.

Olsen, R. C.; McIlwain, C. E.; and Whipple, E. C., Jr.: Observations of Differential Charging Effects on ATS-6, J. Geophys. Res., vol. 86, Aug. 1, 1981, pp. 6809-6819.

Olsen, R. C.; and Purvis, C. K.: Observations of Charging Dynamics of Spacecraft. J. Geophys. Res., vol. 88, July 1, 1983, pp. 5657-5667.

Olsen, R. C.; and Whipple, E. C.: Active Experiments in Modifying Spacecraft Potential: Results from ATS-5 and ATS-6 (UCSD-SP-79-01, Univ. Calif.; NASA Grant NAS5-23481.) NASA CR-159993, 1979.

Olsen, R. C.; and Whipple, E. C.: Operations of the ATS-6 Ion Engine. Spacecraft Charging Technology—1978, NASA CP-2071, 1979, pp. 59-68.

Olsen, R. C.; and Whipple, E. C.: Active Experiments in Modifying Spacecraft Potential: Results from ATS-5 and ATS-6, (UCSD-SP-77-01, Univ. Calif.; NASA Grant NAS5-23481.) NASA CR-152607, 1977.

Olsen, R. C.; Whipple, E. C.; and Purvis, C. K.: Active Modification of the ATS-5 and ATS-6 Spacecraft Potentials. Effect of the Ionosphere on Space and Terrestrial Systems, J. M. Goodman, ed., Naval Research Lab., 1978, pp. 328-336.

Parker, L. W.: Differential Charging of Nonconducting Spacecraft. Presented at the Symposium on the Effects of the Ionosphere on Space and Terrestrial Systems (Arlington, Va.), Jan. 24-26, 1978.

Parker, L. W.: Potential Barriers and Asymmetric Sheaths due to Differential Charging of Nonconducting Spacecraft. AFGL-TR-78-0045, Lee W. Parker, Inc., 1978. (AD-A053618.)

Parker, L. W.: Theory of Electron Emission Effects in Symmetric Probe and Spacecraft Sheaths. AFGL-TR-76-0294, Lee W. Parker, Inc., 1976. (AD-A037538.)

Parker, L. W.: Computer Method for Satellite Plasma Sheath in Steady-State Spherical Symmetry. AFCRL-TR-75-0410, Lee W. Parker, Inc., 1975. (AD-A015066.)

Parker, L. W.: Computer Solutions in Electrostatic Probe Theory. AFAL-TR-72-222, Mt. Auburn Res. Associates, Inc., 1973.

Parker, L. W.; and Whipple, E. C., Jr.: Theory of Spacecraft Sheath Structure, Potential, and Velocity Effects on Ion Measurements by Traps and Mass Spectrometers. J. Geophys. Res., vol. 75, Sept. 1, 1970, pp. 4720-4733.

Parker, L. W.; and Whipple, E. C., Jr.: Theory of a Satellite Electrostatic Probe. Ann. Phys., vol. 44, Aug. 1967, pp. 126-161.

Pedersen, A.; Guyenne, D.; and Hunt, J.; eds.: Spacecraft/Plasma Interactions and Their Influence on Field and Particle Measurements, European Space Agency, ESA-SP-198, 1983.

Pedersen, A.; et al.: Methods for Keeping a Conductive Spacecraft Near the Plasma Potential. Spacecraft/Plasma Interactions and Their Influence on Field and Particle Measurements, A. Pedersen, D. Guyenne, and J. Hunt, eds., European Space Agency, ESA-SP-198, 1983, pp. 185-190.

Pike, C. P.; and Lovell, R. R., eds.: Proceedings of the Spacecraft Charging Technology Conference. NASA TM X-73537, 1977.

Prokopenko, S. M. L; and Laframboise, J. G.: High-Voltage Differential Charging of Geostationary Spacecraft. J. Geophys. Res. vol. 85, no. A8, Aug. 1, 1980, pp. 4125-4131.

Prokopenko, S. M. L.; and Laframboise, J. G.: Prediction of Large Negative Shaded-Side Spacecraft Potentials. Proceedings of the Spacecraft Charging Technology Conference, C. P. Pike and R. R. Lovell, eds., NASA TM X-73537, 1977, pp. 369-387.

Purvis, C. K.: The Role of Potential Barrier Formation in Spacecraft Charging. Spacecraft/Plasma Interactions and Their Influence on Field and Particle Measurements, A. Pedersen, D. Guyenne, and J. Hunt, eds., European Space Agency, ESA-SP-198, 1983, pp. 115-124.

Purvis, C. K.: Configuration Effects on Satellite Charging Response. AIAA Paper 80-0040, Jan. 1980.

Purvis, C. K.: Arc Discharges of Electron-Irradiated Polymers: Results from the Spacecraft Charging Investigation. 1979 Annual Report: Proceedings of the Conference on Electrical Insulation and Dielectric Phenomena, National Academy of Sciences, 1979, pp. 277-283.

Purvis, C. K.: Status of Material Characterization Studies. Spacecraft Charging Technology—1978, NASA CP-2071, 1979, pp. 437-456.

Purvis, C. K.: Jupiter Probe Charging Study. NASA TP-1263, Jan., 1979.

Purvis, C. K.; and Bartlett, R. O.: Active Control of Spacecraft Charging in Space Systems and Their Interactions with Earth's Space Environment, Prog. Astronaut. Aeronaut., vol. 71, H. B. Garrett and C. D. Pike, eds., AIAA, 1980, pp. 299-317.

Purvis, C. K.; Bartlett, R. O.; and DeForest, S. E.: Active Control of Spacecraft Charging on ATS-5 and ATS-6. Proceedings of the Spacecraft Charging Technology Conference, C. P. Pike and R. R. Lovell, eds., NASA TM X-73537, 1977, pp. 107-120.

Purvis, C. K.; and Staskus, J. V.: SCATHA SSPM Charging Response: NASCAP Predictions Compared with Data. Spacecraft Charging Technology—1980, NASA CP-2182, 1981, pp. 592-607.

Purvis, C. K.; Stevens, N. J.; and Olgebay, J. C.: Charging Characteristics of Materials: Comparison of Experimental Results with Simple Analytical Models. Proceedings of the Spacecraft Charging Technology Conference, C. P. Pike and R. R. Lovell, eds., NASA TM X-73537, pp. 459-486.

Purvis, C. K.; et al.: Charging Rates of Metal-Dielectric Structures. Spacecraft Charging Technology—1978, NASA CP-2071, 1979, pp. 507-523.

Purvis, C. K.: Effects of Secondary Yield Parameter Variation on Predicted Equilibrium Potentials of an Object in a Charging Environment. NASA TM-79299, 1979.

Quinn, J.; and McIlwain, C. E.: Bouncing Ion Clusters in the Earth's Magnetosphere. J. Geophys. Res., vol. 84, Dec. 1, 1979, pp. 7365-7370.

Reasoner, D. L.; Lennartsson, W.; and Chappell, C. R.: Relationship Between ATS-6 Spacecraft-Charging Occurrences and Warm Plasma Encounters. Spacecraft Charging by Magnetospheric Plasmas. Prog. Astronaut. Aeronaut., vol. 47, A. Rosen, ed., AIAA, 1976, pp. 89-101.

Reddy, J.: Electron Irradiation Tests on European Meteorological Satellite. Spacecraft Charging Technology—1980, NASA CP-2182, 1981, pp. 835-855.

Rittenhouse, J. B.; and Singletary, J. B.: Space Materials Handbook. NASA SP-3051, 1969.

Robinson, J. W.: Charge Distributions Near Metal-Dielectric Interfaces Before and After Dielectric Surface Flashover. Proceedings of the Spacecraft Charging Technology Conference, C. P. Pike, and R. R. Lovell, eds., NASA TM X-73537, 1977, pp. 503-516.

Robinson, P. A., Jr.; and Holman, A. B.: Pioneer Venus Spacecraft Charging Model. Proceedings of the Spacecraft Charging Technology Conference, C. P. Pike and R. R. Lovell, eds., NASA TM X-73537, 1977, pp. 297-308.

Roche, J. C.; and Purvis, C. K.: Comparison of NASCAP Predictions with Experimental Data. Spacecraft Charging Technology—1978, NASA CP-2071, 1979, pp. 144-157.

Rogers, J. F.: ATS-6 Quartz Crystal Microbalance. IEEE Trans. Aerosp. Electron. Syst., vol. AES-11, Nov. 1975, pp. 1185-1186.

Rose, A.: Concepts in Photoconductivity and Allied Problems. John Wiley, 1963.

Rosen, A., ed.: Spacecraft Charging by Magnetospheric Plasma, Prog. Astronaut. Aeronaut., vol. 47, MIT Press, 1976.

Rosen, A.; et al.: Effects of Arcing due to Spacecraft Charging on Spacecraft Survival. (TRW-33631-6006-RU-00, TRW Defense and Space Systems Group, NASA Contract NAS3-21363.) NASA CR-159593, 1978.

Rosen, A.; et al.: RGA Analysis: Findings Regarding Correlation of Satellite Anomalies with Magnetospheric Substorms and Laboratory Test Results, Rept. 09670-7020-RO-00, TRW Defense and Space Systems, 1972.

Rothwell, P. L.; Rubin, A. G.; and Yates, G. K.: A Simulation Model of Time-Dependent Plasma-Spacecraft Interactions. Proceedings of the Spacecraft Charging Conference, C. P. Pike and R. R. Lovell, eds., NASA TM X-73537, 1977, pp. 389-412.

Rothwell, P. L.; et al.: Simulation of the Plasma Sheath Surrounding a Charged Spacecraft. Spacecraft Charging by Magnetospheric Plasmas, A. Rosen, ed., Prog. Astronaut. Aeronaut., vol. 47, MIT Press, 1976, pp. 121-133.

Rubin, A. G.; and Garrett, H. B.: ATS-5 and ATS-6 Potentials During Eclipse. Spacecraft Charging Technology—1978, NASA CP-2071, 1979, pp. 38-43.

Rubin, A. G.; et al.: A Three-Dimensional Spacecraft Charging Computer Code. Space Systems and Their Interactions with Earth's Space Environment, H. B. Garrett and C. P. Pike, eds., Prog. Astronaut. Aeronaut., vol. 71, AIAA, 1980, pp. 318-336.

Rubin, A. G.; Rothwell, P. L.; and Yates, G. K.: Reduction of Spacecraft Charging Using Highly Emissive Surface Materials. Effect of the Ionosphere on Space and Terrestrial Systems, J. M. Goodman, ed., U.S. Government Printing Office, 1978, pp. 313-316.

Samir, U.; and Willmore, A. P.: The Equilibrium Potential of a Spacecraft in the Ionosphere, Planet. Space Sci., vol. 14, 1966, pp. 1131-1137.

Sanders, N. L.; and Inouye G. T.: Secondary Emission Effects on Spacecraft Charging: Energy Distribution Considerations. Spacecraft Charging Technology—1978, NASA CP-2071, 1979, pp. 747-755.

Sanders, N. L.; and Inouye, G. T.: Voyager Spacecraft Charging Model Calculations. Presented at the Symposium on the Effects of the Ionosphere on Space and Terrestrial Systems, (Arlington, Va.), Jan. 24-26, 1978.

Schnuelle, G. W.; et al.: Simulation of Charging Response of SCATHA (P78-2) Satellite. Spacecraft Charging Technology—1980, NASA CP-2182, 1981, pp. 580-591.

Schnuelle, G. W.; et al.: Charging Analysis of the SCATHA Satellite. Spacecraft Charging Technology—1978, NASA CP-2071, 1979, pp. 123-143.

Sharp, R. D.; et al.: Preliminary Results of a Low-Energy Particle Survey at Synchronous Altitude. J. Geophys. Res., vol. 75, Nov. 1970, pp. 6092-6101.

Shaw, R. R.; Nanevicz, J. E.; and Adamo, R. C.: Observations of Electrical Discharges Caused by Differential Satellite Charging. Spacecraft Charging by Magnetospheric Plasmas, A. Rosen, ed., Prog. Astronaut. Aeronaut., vol. 47, MIT Press, 1976, pp. 61-76.

Singer, S. F., ed.: Interactions of Space Vehicles with an Ionized Atmosphere. Pergamon Press, 1965.

Stang, D. B.; and Purvis, C. K.: Comparison of NASCAP Modeling Results with Lumped-Circuit Analysis. Spacecraft Charging Technology—1980, NASA CP-2182, 1981, pp. 665-683.

Stannard, P. R.; et al.: Validation of the NASCAP Model Using Spaceflight Data. AIAA Paper 82-0269, Jan. 1982.

Stannard P. R.; et al.: Representation and Material Charging Response of GEO Plasma Environments. Spacecraft Charging Technology—1980, NASA CP-2182, 1981, pp. 560-579.

Staskus, J. V.; and Roche, J. C.: Testing of a Spacecraft Model in a Combined Environment Simulator. NASA TM-82723, 1981.

Sternglass, E. J.: Theory of Secondary Electron Emission by High Speed Ions, Phys. Rev., vol. 108, no. 1, Oct. 1, 1957, pp. 1-12.

Sternglass, E. J.: Backscattering of Kilovolt Electrons from Solids. Phys. Rev., vol. 95, no. 2, July 15, 1954, pp. 345-358.

Sternglass, E. J.: Secondary Electron Emission and Atomic Shell Structure. Phys. Rev., vol. 80, no. 5, Dec. 1, 1950, pp. 925-926.

Stevens, N. J.: Use of Charging Control Guidelines for Geosynchronous Satellite Design Studies. Spacecraft Charging Technology—1980, NASA CP-2182, 1981, pp. 789-801.

Stevens, N. J.: Analytical Modeling of Satellites in Geosynchronous Environment. Spacecraft Charging Technology—1980, NASA CP-2182, 1981, pp. 717-729.

Stevens, N. J.: Space Environment Interactions with Biased Spacecraft Surfaces. Space Systems and Their Interactions with Earth's Space Environment, H. B. Garrett and C. P. Pike, eds., Prog. Astronaut. Aeronaut., vol. 71, 1980, pp. 455-476.

Stevens, N. J.; Berkopec, F. D.; Staskus, J. V.; Blech, R. A.; and Narcisco, N. J.: Testing of Typical Spacecraft Materials in a Simulated Substorm Environment. Proceedings of the Spacecraft Charging Technology Conference, C. P. Pike and R. R. Lovell, eds., NASA TM X-73537, 1977, pp. 431-457.

Stevens, N. J.; Klinect, V. W.; and Gore, J. V.: Summary of the CTS Transient Event Counter Data After One Year of Operation. IEEE Trans. Nucl. Sci., vol. NS-24, Dec. 1977, pp. 2270-2275.

Stevens, N. J.; Lovell, R. R.; and Gore, J. V.: Spacecraft-Charging Investigation for the CTS Project. Spacecraft Charging by Magnetospheric Plasmas, A. Rosen, ed., Prog. Astronaut. Aeronaut., vol. 47, AIAA, 1976, pp. 263-275.

Stevens, N. J.; Mills, H. E.; and Orange, L.: Voltage Gradients in Solar Array Cavities as Possible Breakdown Sites in Spacecraft-Charging-Induced Discharges. NASA TM-82710, 1981.

Stevens, N. J.; and Purvis, C. K.: NASCAP Modeling Computations on Large Optics Spacecraft in Geosynchronous Substorm Environment. NASA TM-81395, 1980.

Stevens, N. J.; Purvis, C. K.; and Staskus, J. V.: Insulator Edge Voltage Gradient Effects in Spacecraft Charging Phenomena. IEEE Trans. Nucl. Sci., vol. NS-25, Dec. 1978, pp. 1304-1312.

Stevens, N. J.; Staskus, J. V.; Roche, J. C.; and Mezira, P. F.: Initial Comparison of SSPM Ground Test Results and Flight Data to NASCAP Simulations, NASA TM-81394, 1980.

Stevens, N. J.; Sturman, J. C.; and Berkopec, F. D.: Development of Environmental Charging Effect Monitors for Operational Satellites. Proceedings of the Spacecraft Charging Technology Conference, C. P. Pike and R. R. Lovell, eds., NASA TM X-73537, 1977, pp. 745-751.

Sturman J. C.: Development and Design of Three Monitoring Instruments for Spacecraft Charging. NASA TP-1800, 1981.

Treadaway, M. J.; et al.: The Effects of High-Energy Electrons on the Charging of Spacecraft Dielectrics. IEEE Trans. Nucl. Sci., vol. NS-26, Dec. 1979, pp. 5102-5106.

Tsipouras, P.; and Garrett, H. B.: Spacecraft Charging Model: Two Maxwellian Approximation. AFGL-TR-79-0153, Air Force Geophysics Lab., 1979. (AD-A077907.)

Vampola, A. L.: P78-2 Engineering Overview. Spacecraft Charging Technology—1980, NASA CP-2182, 1981, pp. 439-460.

Van Lint, V. A. J.; et al.: Mechanisms of Radiation Effects in Electronic Materials. Vol. 1, John Wiley, 1980.

Whipple, E. C., Jr.: Modeling of Spacecraft Charging. Proceedings of the Spacecraft Charging Technology Conference, C. P. Pike and R. R. Lovell, eds., NASA TM X-73537, 1977, pp. 225-236.

Whipple, E. C.; Jr.: Theory of the Spherically Symmetric Photoelectron Sheath: A Thick Sheath Approximation and Comparison with the ATS Observation of a Potential Barrier. J. Geophys. Res., vol. 81, Feb. 1, 1976, pp. 601-607.

Whipple, E. C., Jr.: Observation of Photoelectrons and Secondary Electrons Reflected from a Potential Barrier in the Vicinity of ATS-6. J. Geophys. Res., vol. 81, Feb. 1, 1976, pp. 715-719.

Whipple, E. C., Jr.: The Equilibrium Electric Potential of a Body in the Upper Atmosphere and in Interplanetary Space. NASA TM X-55368, 1965.

Whipple, E. C.; et al.: Anomalously High Potentials Observed on ISEE. Spacecraft/Plasma Interactions and Their Influence on Field and Particle Measurements, A. Pedersen, D. Guyenne, and J. Hunt, eds., European Space Agency, ESA-SP-198, 1983, pp. 35-40.

Whipple, E. C.: Potentials of Surfaces in Space. Rep. Prog. Phys., vol. 44, Nov. 1981, pp. 1197–1250.

Whipple, E. C. Jr.; and Olsen, R. C.: Experiments on Regulation of Electric Charge on Space Vehicles. AIAA Paper 79-1506, July 1979.

Whipple, E. C., Jr.; and Parker, L. W.: Theory of an Electron Trap on a Charged Spacecraft. J. Geophys. Res., vol. 74, June 1, 1969, pp. 2962–2971.

Whipple, E. C., Jr.; and Parker, L. W.: Effects of Secondary Electron Emission on Electron Trap Measurements in the Magnetosphere and Solar Wind. J. Geophys. Res., vol. 74, Nov. 1, 1969, pp. 5763–5774.

Whipple, E. C.; Warnock, J. M.; and Winkler, R. H.: Effect of Satellite Potential on Direct Ion Density Measurements Through the Plasmapause. J. Geophys. Res., vol. 79, Jan. 1, 1974, pp. 179–186.

Whittlesey, A. C.: Voyager Electrostatic Discharge Protection Program. International Symposium on Electromagnetic Compatibility, Proceedings, IEEE, 1978, pp. 377–383.

Whittlesey, A.; and Inouye, G.: Voyager Spacecraft Electrostatic Discharge Testing. J. Environ. Sci., vol. 23, Mar.-Apr. 1980, pp. 29–33.

Wilkenfeld, J. M.; Harlacher, B. L.; and Mathews, D.: Development of Electrical Test Procedures for Qualification of Spacecraft Against EID, Vol. 2: Review and Specification of Test Procedures. (IRT-8195-022-1, IRT Corp.; NASA Contract NAS3-21967.) NASA CR-165590, 1982.

Willis, R. F.; and Skinner, D. K.: Secondary Electron Emission Yield Behavior of Polymers. Solid State Commun., vol. 13, no. 6, Sept. 15, 1973, pp. 685–688.

Winckler, J. R.: The Application of Artificial Electron Beams to Magnetospheric Research. Rev. Geophys. Space Phys., vol. 18, Aug. 1980, pp. 659–682.

Worlock, R. M.; et al.: ATS-6 Cesium Bombardment Engine North-South Stationkeeping Experiment, IEEE Trans. Aerosp. Electron. Syst., vol. AES-11, Nov. 1975, pp. 1176–1184.

Wrenn, G. L.; and Heikkila, W. J.: Photoelectrons Emitted from ISIS Spacecraft. Photon and Particle Interactions with Surfaces in Space. R. J. L. Grard, ed., D. Reidel Publ. Co., 1973, pp. 221–230.

Yadlowsky, E. J.; Hazelton, R. C.; and Churchill, R. J.: Puncture Discharge in Surface Dielectrics as Contaminant Sources in Spacecraft Environments. Proceedings of the USAF/NASA International Spacecraft Contamination Conference, J. M. Jemiola, ed., Air Force Materials Lab., NASA CP-2039, 1978, pp. 945–969.

1. Report No.	2. Government Accession No.	3. Recipient's Catalog No.
NASA TP-2361		

4. Title and Subtitle	5. Report Date
Design Guidelines for Assessing and Controlling Spacecraft Charging Effects	September 1984
	6. Performing Organization Code: 506-55-72

7. Author(s)	8. Performing Organization Report No.
Carolyn K. Purvis, Henry B. Garrett, A. C. Whittlesey, and N. John Stevens	E-2073
	10. Work Unit No.

9. Performing Organization Name and Address	11. Contract or Grant No.
National Aeronautics and Space Administration Lewis Research Center Cleveland, Ohio 44135	
	13. Type of Report and Period Covered: Technical Paper

12. Sponsoring Agency Name and Address	14. Sponsoring Agency Code
National Aeronautics and Space Administration Washington, D.C. 20546	

15. Supplementary Notes

C. K. Purvis, Lewis Research Center; H. B. Garrett and A. Whittlesey, California Institute of Technology, Jet Propulsion Laboratory, Pasadena, California; N. John Stevens, Hughes Aircraft Company, El Segundo, California.

16. Abstract

Experience has indicated a need for uniform criteria, or guidelines, to be used in all phases of spacecraft design. Accordingly, guidelines have been developed for the control of absolute and differential charging of spacecraft surfaces by the lower energy (less than approximately 50 keV) space charged-particle environment. Interior charging due to higher energy particles was not considered. This document is to be regarded as a guide to good design practices for assessing and controlling charging effects. It is not a NASA or Air Force mandatory requirement unless specifically included in project specifications. It is expected, however, that this document, revised as experience may indicate, will provide uniform design practices for all space vehicles.

17. Key Words (Suggested by Author(s))	18. Distribution Statement
Spacecraft charging Geosynchronous spacecraft design Electromagnetic compatibility	Unclassified - Unlimited STAR Category 18

19. Security Classif. (of this report)	20. Security Classif. (of this page)	21. No. of pages	22. Price*
Unclassified	Unclassified	44	A03

*For sale by the National Technical Information Service, Springfield, Virginia 22161

NASA-Langley, 1984